## Discussion

CAR, as well as PXR, regulates the expression of genes involved in the metabolism and transport of xenobiotics and endobiotics [20–22]. It is possible that functional alterations resulting from genetic polymorphisms may influence drug metabolism and therapeutic outcomes. To date, several non-synonymous SNPs that affect the transactivation ability of human PXR have been reported [19,23,24]. These PXR variants might cause variations between individuals in their responses to drugs. CAR is a close relative of PXR, with which it shares several overlapping properties. However, little is known about SNPs in *CAR*. Recently, we found one non-synonymous SNP in exon 4 that induces a Val133Gly substitution in the Japanese population [17]. In this study, we sequenced the *CAR* gene in an additional set of Japanese subjects.

In the coding region for CAR, we found a total of four SNPs with changes that would lead to amino acid alterations (Val133Gly, His246Arg, Leu308Pro, and Asn323Ser). These variants, along with wild-type CAR, were transiently expressed in COS-7 cells, and their transactivation abilities were determined by utilizing the *CYP3A4* promoter/enhancer luciferase reporter gene system in the presence or absence of an agonistic ligand, CITCO. The His246Arg variant showed a dramatically decreased constitutive activity and was no longer activated by CITCO. The Leu308Pro variant also had a reduced constitutive transactivation ability but retained its responsiveness to the ligand. The other two variants, Val133Gly and Asn323Ser, showed similar levels of constitutive activity to that of the wild-type CAR (Fig. 3). The responsiveness to CITCO of the two variants were also retained (Fig. 4). As shown in Fig. 4 and also in our recent study [18], the increasing effect of CITCO is relatively small (at most 2-fold even at 10 μM) in the reporter gene assay using transfected cell lines, which makes it difficult to determine the reliable EC50 or affinity for CITCO. To improve accuracy, a different approach, e.g., a usage of primary hepatocyte cultures, might be warranted.

All four of these amino acid variations were located in the LBD. The LBD of most nuclear receptors is a multifunctional domain that mediates ligand binding, dimerization with RXR, interactions with co-activator proteins, nuclear localization, and most importantly, transactivation functions via the C-terminal transactivation domain AF2. The X-ray crystal structure of CAR shows that the LBD is composed of 11 α-helices, two $3_{10}$ helixes, and three β-strands, while Val133, His246, Leu308, and Asn323 map to helices H2, H7, H10, and H10, respectively [25–27]. H7 contributes to the ligand binding pocket and participates in interactions with the ligand [27]. Recently, it has been reported that H7 is involved in the selectivity for CAR ligands [28]. This finding might explain the observation that the His246Arg variant lacks responsiveness to CITCO. Activation of nuclear receptors requires that the AF2 helix be precisely positioned. In CAR, H10 interacts with the AF2 helix to maintain the active conformation of the protein [25]. The reduced transactivation activities of the His246Arg and Leu308Pro variants might be due to conformational changes of AF2 resulting from the amino acid alterations. Thus, it is possible that His246 and Leu308 play an important role in stabilizing the active conformation of the receptor.

CAR regulates a number of genes encoding enzymes involved in xenobiotic/endobiotic metabolism, conjugation, and transport of small hydrophobic substrates. Moreover, recent studies have indicated that CAR participates in bilirubin clearance [5], bile acid detoxification [29], and adaptive responses to nutrition stress [6]. The physiological importance of CAR is becoming increasingly apparent. Thus, variations of CAR resulting in functional alterations may have serious impacts on pharmacological and physiological responses of the target genes.

In conclusion, we functionally characterized four naturally occurring CAR variants. The variant His246Arg showed a marked reduction of constitutive activity and failed to respond to CITCO. Although the Leu308Pro variant retained normal responsiveness to CITCO, its constitutive transactivation ability was significantly reduced.

## Acknowledgments

We thank Ms. Chie Knudsen for her secretarial assistance. This study was supported in part by the Program for the Promotion of Fundamental Studies in Health Sciences and in part by the Program for the Promotion of Studies in Health Sciences of the Ministry of Health, Labor and Welfare of Japan.

## References

[1] M. Baes, T. Gulick, H.S. Choi, M.G. Martinoli, D. Simha, D.D. Moore, A new orphan member of the nuclear hormone receptor superfamily that interacts with a subset of retinoic acid response elements, Mol. Cell. Biol. 14 (1994) 1544–1552.
[2] V. Giguere, Orphan nuclear receptors: from gene to function, Endocr. Rev. 20 (1999) 689–725.
[3] A. Ueda, H.K. Hamadeh, H.K. Webb, Y. Yamamoto, T. Sueyoshi, C.A. Afshari, J.M. Lehmann, M. Negishi, Diverse roles of the nuclear orphan receptor CAR in regulating hepatic genes in response to phenobarbital, Mol. Pharmacol. 61 (2002) 1–6.
[4] C. Handschin, U.A. Meyer, Induction of drug metabolism: the role of nuclear receptors, Pharmacol. Rev. 55 (2003) 649–673.
[5] W. Huang, J. Zhang, S.S. Chua, M. Qatanani, Y. Han, R. Granata, D.D. Moore, Induction of bilirubin clearance by the constitutive androstane receptor (CAR), Proc. Natl. Acad. Sci. USA 100 (2003) 4156–4161.

[6] J.M. Maglich, J. Watson, P.J. McMillen, B. Goodwin, T.M. Willson, J.T. Moore, The nuclear receptor CAR is a regulator of thyroid hormone metabolism during caloric restriction, J. Biol. Chem. 279 (2004) 19832–19838.
[7] T. Sueyoshi, T. Kawamoto, I. Zelko, P. Honkakoski, M. Negishi, The repressed nuclear receptor CAR responds to phenobarbital in activating the human CYP2B6 gene, J. Biol. Chem. 274 (1999) 6043–6046.
[8] B. Goodwin, E. Hodgson, D.J. D'Costa, G.R. Robertson, C. Liddle, Transcriptional regulation of the human CYP3A4 gene by the constitutive androstane receptor, Mol. Pharmacol. 62 (2002) 359–365.
[9] S.S. Ferguson, E.L. LeCluyse, M. Negishi, J.A. Goldstein, Regulation of human CYP2C9 by the constitutive androstane receptor: discovery of a new distal binding site, Mol. Pharmacol. 62 (2002) 737–746.
[10] S. Gerbal-Chaloin, M. Daujat, J.M. Pascussi, L. Pichard-Garcia, M.J. Vilarem, P. Maurel, Transcriptional regulation of CYP2C9 gene. Role of glucocorticoid receptor and constitutive androstane receptor, J. Biol. Chem. 277 (2002) 209–217.
[11] Y. Chen, S.S. Ferguson, M. Negishi, J.A. Goldstein, Identification of constitutive androstane receptor and glucocorticoid receptor binding sites in the CYP2C19 promoter, Mol. Pharmacol. 64 (2003) 316–324.
[12] J. Sugatani, H. Kojima, A. Ueda, S. Kakizaki, K. Yoshinari, Q.H. Gong, I.S. Owens, M. Negishi, T. Sueyoshi, The phenobarbital response enhancer module in the human bilirubin UDP-glucuronosyltransferase UGT1A1 gene and regulation by the nuclear receptor CAR, Hepatology 33 (2001) 1232–1238.
[13] B.M. Forman, I. Tzameli, H.S. Choi, J. Chen, D. Simha, W. Seol, R.M. Evans, D.D. Moore, Androstane metabolites bind to and deactivate the nuclear receptor CAR-beta, Nature 395 (1998) 612–615.
[14] J.M. Maglich, D.J. Parks, L.B. Moore, J.L. Collins, B. Goodwin, A.N. Billin, C.A. Stoltz, S.A. Kliewer, M.H. Lambert, T.M. Willson, J.T. Moore, Identification of a novel human constitutive androstane receptor (CAR) agonist and its use in the identification of CAR target genes, J. Biol. Chem. 278 (2003) 17277–17283.
[15] S.S. Auerbach, R. Ramsden, M.A. Stoner, C. Verlinde, C. Hassett, C.J. Omiecinski, Alternatively spliced isoforms of the human constitutive androstane receptor, Nucleic Acids Res. 31 (2003) 3194–3207.
[16] J.M. Pascussi, M. Busson-Le Coniat, P. Maurel, M.J. Vilarem, Transcriptional analysis of the orphan nuclear receptor constitutive androstane receptor (NR1I3) gene promoter: identification of a distal glucocorticoid response element, Mol. Endocrinol. 17 (2003) 42–55.
[17] S. Ikeda, K. Kurose, S. Ozawa, K. Sai, R. Hasegawa, K. Komamura, K. Ueno, S. Kamakura, M. Kitakaze, H. Tomoike, T. Nakajima, K. Matsumoto, H. Saito, Y. Goto, H. Kimura, M. Katoh, K. Sugai, N. Minami, K. Shirao, T. Tamura, N. Yamamoto, H. Minami, A. Ohtsu, T. Yoshida, N. Saijo, Y. Saito, J. Sawada, Twenty-six novel single nucleotide polymorphisms and their frequencies of the NR1I3 (CAR) gene in a Japanese population, Drug Metab. Pharmacokinet. 18 (2003) 413–418.
[18] H. Jinno, T. Tanaka-Kagawa, N. Hanioka, S. Ishida, M. Saeki, A. Soyama, M. Itoda, T. Nishimura, Y. Saito, S. Ozawa, M. Ando, J. Sawada, Identification of novel alternative splice variants of human constitutive androstane receptor and characterization of their expression in the liver, Mol. Pharmacol. 65 (2004) 496–502.
[19] S. Koyano, K. Kurose, Y. Saito, S. Ozawa, R. Hasegawa, K. Komamura, K. Ueno, S. Kamakura, M. Kitakaze, T. Nakajima, K. Matsumoto, A. Akasawa, H. Saito, J. Sawada, Functional characterization of four naturally occurring variants of human pregnane X receptor (PXR): one variant causes dramatic loss of both DNA binding activity and the transactivation of the CYP3A4 promoter/enhancer region, Drug Metab. Dispos. 32 (2004) 149–154.
[20] P. Honkakoski, T. Sueyoshi, M. Negishi, Drug-activated nuclear receptors CAR and PXR, Ann. Med. 35 (2003) 172–182.
[21] P. Wei, J. Zhang, D.H. Dowhan, Y. Han, D.D. Moore, Specific and overlapping functions of the nuclear hormone receptors CAR and PXR in xenobiotic response, Pharmacogenomics J. 2 (2002) 117–126.
[22] T.M. Willson, S.A. Kliewer, PXR, CAR and drug metabolism, Nat. Rev. Drug Discov. 1 (2002) 259–266.
[23] E. Hustert, A. Zibat, E. Presecan-Siedel, R. Eiselt, R. Mueller, C. Fuss, I. Brehm, U. Brinkmann, M. Eichelbaum, L. Wojnowski, O. Burk, Natural protein variants of pregnane X receptor with altered transactivation activity toward CYP3A4, Drug Metab. Dispos. 29 (2001) 1454–1459.
[24] J. Zhang, P. Kuehl, E.D. Green, J.W. Touchman, P.B. Watkins, A. Daly, S.D. Hall, P. Maurel, M. Relling, C. Brimer, K. Yasuda, S.A. Wrighton, M. Hancock, R.B. Kim, S. Strom, K. Thummel, C.G. Russell, J.R. Hudson Jr., E.G. Schuetz, M.S. Boguski, The human pregnane X receptor: genomic structure and identification and functional characterization of natural allelic variants, Pharmacogenetics 11 (2001) 555–572.
[25] K. Suino, L. Peng, R. Reynolds, Y. Li, J.Y. Cha, J.J. Repa, S.A. Kliewer, H.E. Xu, The nuclear xenobiotic receptor CAR: structural determinants of constitutive activation and heterodimerization, Mol. Cell 16 (2004) 893–905.
[26] L. Shan, J. Vincent, J.S. Brunzelle, I. Dussault, M. Lin, I. Ianculescu, M.A. Sherman, B.M. Forman, E.J. Fernandez, Structure of the murine constitutive androstane receptor complexed to androstenol: a molecular basis for inverse agonism, Mol. Cell 16 (2004) 907–917.
[27] R.X. Xu, M.H. Lambert, B.B. Wisely, E.N. Warren, E.E. Weinert, G.M. Waitt, J.D. Williams, J.L. Collins, L.B. Moore, T.M. Willson, J.T. Moore, A structural basis for constitutive activity in the human CAR/RXRalpha heterodimer, Mol. Cell 16 (2004) 919–928.
[28] J. Jyrkkarinne, B. Windshugel, J. Makinen, M. Ylisirnio, M. Perakyla, A. Poso, W. Sippl, P. Honkakoski, Amino acids important for ligand specificity of the human constitutive androstane receptor, J. Biol. Chem. 280 (2005) 5960–5971.
[29] S.P. Saini, J. Sonoda, L. Xu, D. Toma, H. Uppal, Y. Mu, S. Ren, D.D. Moore, R.M. Evans, W. Xie, A novel constitutive androstane receptor-mediated and CYP3A-independent pathway of bile acid detoxification, Mol. Pharmacol. 65 (2004) 292–3003.

# Different Effects of Desipramine on Bufuralol 1″-Hydroxylation by Rat and Human CYP2D Enzymes

Takashi ISOBE,[a] Hiroyuki HICHIYA,[a] Nobumitsu HANIOKA,[a] Shigeo YAMAMOTO,[b] Sumio SHINODA,[c] Yoshihiko FUNAE,[d] Tetsuo SATOH,[e] Shigeru YAMANO,[f] and Shizuo NARIMATSU*,[a]

[a] *Laboratory of Health Chemistry, Faculty of Pharmaceutical Sciences, Okayama University;* [b] *Laboratory of Biomolecular Sciences, Faculty of Pharmaceutical Sciences, Okayama University;* [c] *Laboratory of Environmental Hygine, Faculty of Pharmaceutical Sciences, Okayama University; 1–1–1 Tsushima-naka, Okayama 700–8530, Japan:* [d] *Laboratory of Chemistry, Osaka City University Medical School; 1–4–54 Asahimachi, Abeno-ku, Osaka 545–8585, Japan:* [e] *Human Animal Bridge Discussion Group; 2802–1 Hiratsuka, Shiroi, Chiba 270–8601, Japan: and* [f] *Department of Hygienic Chemistry, Faculty of Pharmaceutical Sciences, Fukuoka University; 8–19–1 Nanakuma, Jonan-ku, Fukuoka 814–0180, Japan.* Received November 15, 2004; accepted January 13, 2005

**Inhibitory effects of desipramine (DMI) on rat and human CYP2D enzymes were studied using bufuralol (BF) 1″-hydroxylation as an index. Inhibition was examined under the following two conditions: 1) DMI was co-incubated with BF and NADPH in the reaction mixture containing rat or human liver microsomes or yeast cell microsomes expressing rat CYP2D1, CYP2D2 or human CYP2D6 (co-incubation); 2) DMI was preincubated with NADPH and the same enzyme sources prior to adding the substrate (preincubation). When either rat liver microsomes or recombinant CYP2D2 was employed, the preincubation with DMI (0.3 μM) caused a greater inhibition of BF 1″-hydroxylation than the co-incubation did, whereas BF 1″-hydroxylation by rat CYP2D1 was not markedly affected under the same conditions. The inhibitory effect of DMI on BF 1″-hydroxylation by human liver microsomal fractions or recombinant CYP2D6 was much lower than that on the hydroxylation by rat liver microsomes or CYP2D2. Kinetic studies demonstrated that the inhibition-type changed from competitive for the co-incubation to noncompetitive for the preincubation in the case of CYP2D2, whereas the inhibition-type was competitive for both the co-incubation and the preincubation in the case of CYP2D6. Furthermore, the loss of activity of rat CYP2D2 under the preincubation conditions followed pseudo-first-order kinetics. Binding experiments employing the recombinant enzymes and [$^3$H]-DMI revealed that CYP2D2 and CYP2D6 were the only prominent proteins to which considerable radioactive DMI metabolite(s) bound. These results indicate that rat CYP2D2 biotransforms DMI into reactive metabolite(s), which covalently bind to CYP2D2, resulting in inactivation of the enzyme. In contrast, human CYP2D6 may also biotransform DMI into some metabolite(s) that covalently bind to CYP2D6, but that do not inactivate the enzyme.**

**Key words** desipramine; CYP2D2; CYP2D6; reactive metabolite; binding; inactivation

Imipramine (IMI) and desipramine (DMI) are tricyclic antidepressants that are widely used clinically. As shown in Fig. 1, IMI is oxidized by cytochrome P450 (CYP) mainly *via* two pathways: side-chain *N*-demethylation and aromatic ring 2-hydroxylation, forming DMI and 2-hydroxyimipramine (2-OH-IMI), respectively.[1] DMI and 2-OH-IMI further undergo 2-hydroxylation and *N*-demethylation, respectively, forming 2-hydroxy-DMI as the common metabolite (Fig. 1). In the human liver, CYP2D6 is mainly responsible for IMI 2-hydroxylation whereas CYP2C19 and CYP1A2 are involved in *N*-demethylation.[2,3]

It has been reported that repeated administration of IMI to rats changed hepatic CYP-dependent monooxygenase activities.[4—6] We have also found that repetitive oral administration of IMI to rats caused a decrease in hepatic microsomal CYP2D-dependent reactions such as debrisoquine 4-hydroxylation, bunitrolol 4-hydroxylation, lidocaine 3-hydroxylation and propranolol 4-, 5- and 7-hydroxylations.[7] We have proposed that binding of a reactive metabolite of IMI to rat CYP2D enzyme(s) resulted in the decreased enzyme activities.[7] As a possible mechanism, we speculated that an epoxy metabolite of IMI (1,2- or 2,3-epoxide) was involved in the inactivation of rat CYP2D enzyme(s).[7,8]

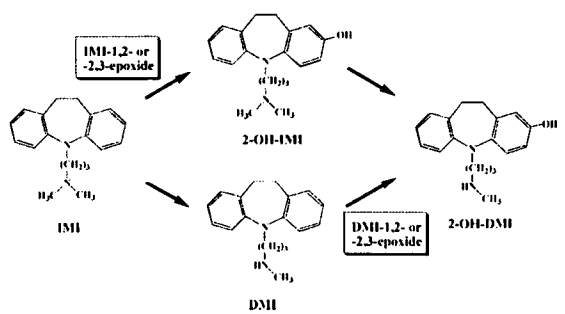


Fig. 1. Parallel Metabolic Pathways of the Conversion of IMI to 2-OH-DMI

If the epoxy metabolite(s) of IMI are responsible for the inactivation, DMI would also inactivate the rat CYP2D enzyme(s). Because several CYP2D enzymes are known to be expressed in the rat liver,[9] it is interesting to know what kind of CYP2D isoenzyme(s) are inhibited by IMI or DMI. Furthermore, there is a possibility that CYP2D6, a human functional CYP2D enzyme, is also inactivated by IMI and DMI in a similar manner. The present study was thus conducted to examine these possibilities using radiolabeled and unlabeled DMI and recombinant human and rat CYP2D enzymes.

## MATERIALS AND METHODS

**Materials** DMI as the hydrochloride and propranolol racemate as the hydrochloride were obtained from Sigma Chemical Co. (St. Louis, MO, U.S.A.); bufuralol (BF) and

* To whom correspondence should be addressed. e-mail: shizuo@pharm.okayama-u.ac.jp

1″-hydroxybufuralol (1″-OH-BF) (both as hydrochlorides) were from Daiichi Pure Chemical Co. (Tokyo, Japan); dithiothreitol was from Nacalai Tesque (Kyoto, Japan); [$^3$H]-labeled DMI (specific activity 2.96 TBq/mmol, radiochemical purity above 97%) was from NEN Life Science Products, Inc. (Boston, MA, U.S.A.); glucose 6-phosphate (G-6-P), G-6-P dehydrogenase and NADPH were from Oriental Yeast Co., Ltd. (Tokyo, Japan). All other chemicals and organic solvents used were of analytical grade.

**Rat and Human Liver Microsomes** Male Wistar rats (6 weeks old) were purchased from Clea Japan Co. (Shizuoka, Japan). Liver microsomal fractions were prepared from rats by a published method.[10] Human liver microsomal fractions ($n$=3, all male Caucasians from 25 to 56 years old) were supplied from Human and Animal Bridge Discussion Group (HAB) (Chiba, Japan). This study was approved by the Ethics Committee of the Faculty of Pharmaceutical Sciences, Okayama University.

**Recombinant CYP2D Enzymes** Recombinant rat CYP2D2[9] and human CYP2D6[11] were expressed in yeast cells (*Saccharomyces cerevisiae* AH-22 strain) according to methods previously reported. Rat CYP2D2-G45V mutant protein, which has valine instead of glycine at position 45 of CYP2D2, was expressed in yeast cells as reported elsewhere.[12] The contents of CYP2D enzymes in yeast cell microsomal fractions were 52.8, 92.0, 2.1 and 6.5 pmol/mg protein for CYP2D6, CYP2D1, CYP2D2 and CYP2D2-G45V, respectively.

**Incubation of Rat or Human Liver Microsomal Fractions with IMI or DMI** The inhibitory effects of DMI on rat or human liver microsomal BF 1″-hydroxylation were examined under three conditions as summarized in Chart 1a—c: rat or human liver microsomal fraction (0.5 mg protein) was added to ice-cold reaction medium (final volume 500 $\mu$l) in a brown glass conical tube (10 ml) with a glass stopper containing 5 mM G-6-P, 1 IU G-6-P dehydrogenase, 5 mM $MgCl_2$, 0.1 mM EDTA, 0.5 mM NADPH in 100 mM potassium phosphate buffer (pH 7.4) and preincubated for 5 min. NADPH (final concentration 0.5 mM) with or without DMI (final concentration 0.3 $\mu$M for the rat enzyme sources and 3.0 $\mu$M for the human enzyme sources) was added to the equilibrated mixture and allowed to incubate at 37 °C for 2 min, after which BF (final concentration 0.5 $\mu$M) was added and BF 1″-hydroxylation was allowed to proceed for 1 min. After the reaction was stopped by adding 1 ml of 1 M NaOH aqueous solution and vortex mixing, 1 ml of 1 M sodium carbonate buffer (pH 9.6) and propranolol racemate (100 nmol, internal standard) were added, and 1″-OH-BF was extracted into 5 ml of ethyl acetate by vigorous shaking. After centrifugation (1000×$g$ for 10 min) 4 ml of the organic layer was taken and evaporated to dryness under $N_2$ stream. The residue was dissolved in 100 $\mu$l of the HPLC mobile phase described below, and an aliquot (10 $\mu$l) was subjected to HPLC under the conditions described below. In the case of recombinant enzymes, yeast cell microsomal fractions containing 3 pmol of rat or human recombinant CYP were employed. In preliminary experiments, linearity of product formation as a function of time was confirmed for each case.

**HPLC Conditions** A Shimadzu LC-9A liquid chromatograph equipped with a Shimadzu RF-10A fluorescence detector, a Rheodyne Model 7125 injector and a Shimadzu C-R4A Chromatopac data processor were used with the following: column, Inertsil ODS (4.6 mm×250 mm, GL Science, Tokyo, Japan); mobile phase, acetonitrile/20 mM perchloric acid (pH 2.5) (35 : 65, by volume) at a flow rate of 1.5 ml/min; detection, fluorescence 252/302 nm (excitation/emission).

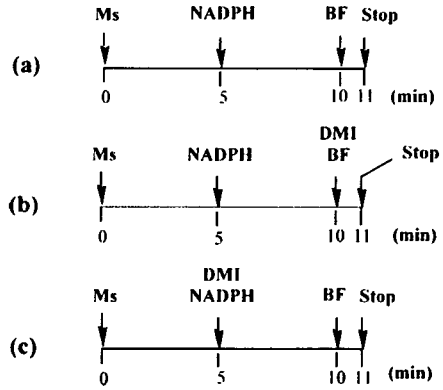


Chart 1

**Kinetic Analysis** Kinetic studies of BF 1″-hydroxylation by the rat liver microsomes or the recombinant CYP2D enzymes were performed using a BF concentration range from 0.2 to 20 $\mu$M and DMI concentration of 0.3 $\mu$M for the rat enzymes and 3.0 $\mu$M for the human enzyme. Apparent Michaelis constant ($K_m$) and maximal velocity ($V_{max}$) were analyzed using the nonlinear least squares regression analysis program MULTI.[13] Inhibition experiments were analyzed by fitting expressions describing competitive inhibition (Eq. 1) and noncompetitive inhibition (Eq. 2) using the same program mentioned above.

$$v = \frac{V_{max} \cdot S}{K_m + (K_m / K_i) \cdot I + S} \quad (1)$$

$$v = \frac{K_i \cdot V_{max} \cdot S}{(K_i + I)(K_m + S)} \quad (2)$$

where $v$ is the rate of formation of metabolite, $V_{max}$ is the maximum rate of metabolite formation, $S$ is the substrate concentration, $K_m$ is the Michaelis constant, $I$ is the inhibitor concentration and $K_i$ is the inhibition constant.

**Inactivation of CYP2D2** Microsomes from yeast cells expressing CYP2D2 were preincubated with various concentrations of DMI (0, 0.3, 1.0, 2.0, 5.0 $\mu$M) at 37 °C for an appropriate time (0, 0.5, 1, 1.5, 2 min) in the presence of NADPH (0.5 mM). After the preincubation, BF 1″-hydroxylase activities of the preincubated microsomes were assayed as described above. The initial rate constant for the inactivation ($K_{obs}$) was obtained as slopes of initial linear phase plotting logarithm of remaining activity against the preincubation time. The maximum rate constant for inactivation ($K_{inact}$) and the dissociation constant for the enzyme-inactivation ($K_I$) were determined according to the published method.[14]

**Binding Studies** The yeast cell microsomal fraction expressing CYP2D2 or CYP2D6 (50 pmol) was added to equilibrated incubation mixture containing the same ingredients as described above in the enzyme assay, and preincubated at 37 °C for 5 min. DMI (final concentration 10 $\mu$M, 3600000 dpm) was then added, and the mixture was incu-

bated at 37 °C for 30 min in the presence or absence of NADPH (final concentration 0.5 mM). The entire sample mixture was transferred into a dialysis tube, and dialyzed at 4 °C for 6 h against 50 mM Tris–HCl buffer (pH 7.4) containing 20% glycerol, 0.1 mM EDTA and 1 mM dithiothreitol (500 ml×2).

A portion of the dialyzed sample (110 μl) was solubilized and subjected to SDS-PAGE using a 10% slab-gel. The gel was stained with Coomassie Brilliant Blue, and cut into 2-mm strips. The gel strips were then solubilized with hydrogen peroxide, and the radioactivity of the samples was measured using a liquid scintillation counter (LSC-3100, Aloka Co., Tokyo, Japan). The scintillation medium consisted of one volume of Triton X-100 and two volumes of toluene phosphor including 4 g of 2,5-diphenyloxazole and 100 mg of 1,4-bis[2-(4-methyl-5-phenyloxazolyl)] benzene per liter of toluene.

A small portion (10 μl) of the dialyzed sample was subjected to SDS-PAGE using a 10% slab-gel. After electrophoresis, proteins in the gel were transblotted to a PVDF membrane and the CYP2D protein was probed by Western blot analysis using polyclonal antibodies (rabbit IgG) raised against CYP2D1 according to a published method.[15] Various amounts of the recombinant CYP2D enzyme were electrophoresed and transferred to the same membrane, and calibration curves were made by scanning the protein bands corresponding to the CYP2D enzyme using NIH Image (version 1.2) installed in a Power Macintosh G4 equipped with an Epson CC-550L scanner. The localization of the radiolabeled CYP2D enzymes on the PVDF membrane and their radioactivity were measured by imaging analysis with the BAS2000 system (Fuji Film, Co., Tokyo, Japan). The PVDF membrane on which radioactive DMI metabolite(s)-bound proteins were transblotted and another PVDF membrane on which various amounts of [$^3$H]-DMI were spotted were attached to an imaging plate (Fuji Film, Co) and exposed for 2 weeks. Then the imaging plate was scanned using the BAS2000 system, and the radioactivity of the CYP2D2 or CYP2D6 protein band on the membrane was calculated on the basis of the calibration curves.

**Others** Protein concentrations were determined by the method of Lowry *et al.*[16] Total holo-CYP content was spectrophotometrically measured from reduced carbon monoxide (CO) spectra according to the method of Omura and Sato[10] using 91 $mM^{-1}cm^{-1}$ as an absorption coefficient. Statistical significance was calculated with Student's *t*-test using Prism version 3.0 (Graph Pad Software, San Diego, CA, U.S.A.), and differences were considered to be statistically significant when $p$ was $<0.05$.

## RESULTS

**Comparison of Inhibitory Effects of DMI on BF 1″-Hydroxylation by Rat and Human Liver Microsomes and Recombinant CYP Enzymes** In our previous report, we proposed that rat liver microsomal CYP2D enzyme(s) might be inactivated by reactive intermediate(s) formed during IMI metabolism.[8] We thought similarly that CYP2D2 might be a target enzyme that is inactivated during the metabolism of DMI in rat liver microsomes. As the first stage of the present study to test this possibility, we thus compared the inhibitory effects of DMI on BF 1″-hydroxylation between rat liver microsomes (Fig. 2A) and yeast cell microsomes expressing CYP2D1 (Fig. 2B) or CYP2D2 (Fig. 2C) using a DMI concentration of 0.3 μM and a BF concentration of 0.5 μM.

These concentrations of the inhibitor and substrate were chosen to distinguish the inhibition-types of DMI for BF 1″-hydroxylation as clearly as possible, because preliminary

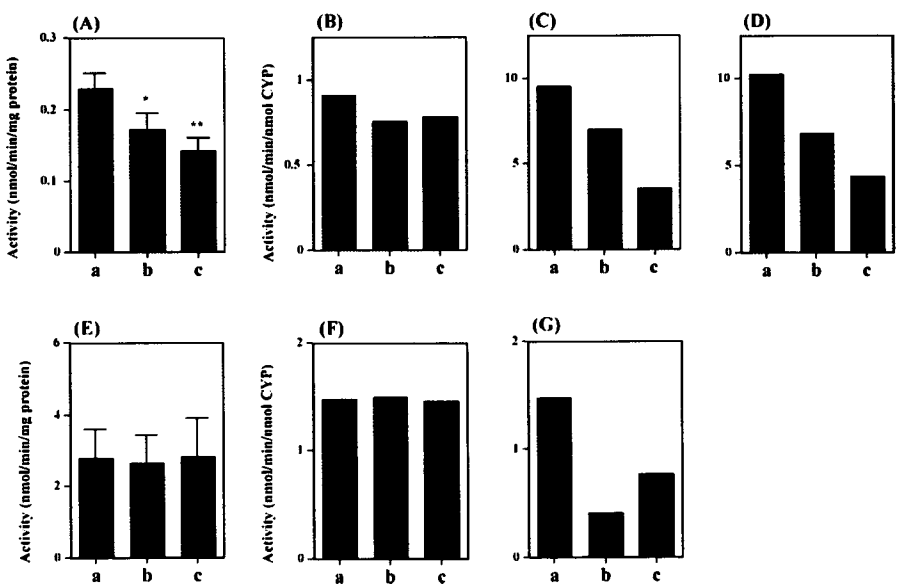


Fig. 2. Comparison of the Inhibitory Effects of DMI on BF 1″-Hydroxylation by Rat or Human Liver Microsomes or Yeast Cell Microsomes Expressing Recombinant CYP Enzymes

The reaction mixtures (final 500 μl) containing various enzyme sources were incubated with BF (0.5 μM) in the presence or absence of DMI (0.3 μM) under the conditions given in Charts 1a, b and c. The enzyme sources were; (A) rat liver microsomes, (B) yeast cell microsomes expressing rat CYP2D2, (C) yeast cell microsomes expressing rat CYP2D2-G45V, (D) human liver microsomes, (E) and (F) yeast cell microsomes expressing human CYP2D6. The concentration of DMI was 0.3 μM except in (F) (3.0 μM). Each value in (A) and (E) is the mean±S.D. ($n$=3). Each value in (B), (C), (D), (F) and (G) is the mean value of two independent determinations. Significantly different from the control (a): $*p<0.05$, $**p<0.01$.

studies indicated that most of 0.3 $\mu$M DMI disappeared from the reaction mixture during a 2 min incubation and at least 50% of 0.5 $\mu$M BF remained after a 1 min incubation under the conditions employed. The co-incubation of BF with DMI significantly inhibited rat hepatic microsomal BF 1″-hydroxylation (Fig. 2A-b) and the preincubation of microsomes with DMI in the presence of NADPH caused a greater inhibition (Fig. 2A-c).

When the recombinant CYP2D1 was used as enzyme source, DMI did not exhibit any clear inhibitory effect on BF 1″-hydroxylase activity (Fig. 2B). On the other hand, DMI produced a greater inhibition of BF 1″-hydroxylation by recombinant CYP2D2 (Fig. 2C). The preincubation of DMI with yeast cell microsomes expressing CYP2D2 in the presence of the cofactor suppressed the activity to 37% of the control level (Fig. 2C-c).

It has been reported that three CYP2D enzymes (CYP2D1, CYP2D2 and CYP2D3) are expressed in the rat liver, and that the microsomal contents of functional CYP2D2 are much lower than those of CYP2D1 and CYP2D3.[17] We recently found that the difference of amino acid residues at positions 43 (tryptophan for CYP2D1 and leucine for CYP2D2) and 45 (valine for CYP2D1 and glycine for CYP2D2) within or near the proline-rich region of the N-terminal region causes the difference in the microsomal functional P450 contents between CYP2D1 and CYP2D2.[12] In that study, we prepared recombinant CYP2D2-G45V having valine instead of glycine-45 and found that the yeast cell microsomal content of the functional holoprotein, P450, was 2- to 3-fold that of wild-type CYP2D2.[12] In the present study, DMI showed a similar inhibition profile for BF 1″-hydroxylation by the wild-type CYP2D2 (Fig. 2C) and by the mutant CYP2D2 (Fig. 2D). Therefore, the inhibitory properties of DMI for CYP2D2 and CYP2D2-G45V are thought to be essentially the same. On the basis of these results, CYP2D2-G45V was used as CYP2D2 in further experiments.

The inhibitory properties of DMI were also examined for human liver microsomes (Fig. 2E) and for yeast cell microsomes expressing recombinant human CYP2D6 (Figs. 2F, G). Interestingly, DMI (0.3 $\mu$M) did not cause any inhibitory effect on BF 1″-hydroxylation by either the human liver microsomes (Fig. 2E) or the recombinant CYP2D6 (Fig. 2F). When a 10-times higher concentration of DMI (3 $\mu$M) was employed, a considerable inhibition was observed (Fig. 2G). These results indicate that the inhibitory effect of DMI on BF 1″-hydroxylation is much stronger with CYP2D2 than with CYP2D1 and CYP2D6.

**Kinetic Studies of the Inhibition by DMI of BF 1″-Hydroxylation by Rat and Human Liver Microsomes and by the Recombinant CYP2D Enzymes** Figure 3 shows typical Lineweaver-Burk plots for the inhibition of BF 1″-hydroxylation by rat liver microsomes (A), CYP2D2 (B) and CYP2D6 (C). In plots in (A) and (B), the co-incubation of DMI and BF yielded a competitive-type inhibition, whereas the preincubation of DMI with rat liver microsomes and CYP2D2 in the presence of NADPH changed the inhibition-type from competitive to noncompetitive. The calculated kinetic parameters are summarized in Table 1.

These results demonstrate that BF 1″-hydroxylation was inhibited competitively when rat CYP2D2 was co-incubated with DMI and BF in the presence of NADPH (Chart 1b) and noncompetitively when the enzyme was preincubated with DMI and NADPH before the incubation with BF (Chart 1c). The $K_i$ value for the recombinant CYP2D2 was 0.3 $\mu$M, which was lower than that (0.6 $\mu$M) for the rat liver microsomes. It is possible that the rat liver microsomes contain not

Table 1. Kinetic Parameters of BF 1″-Hydroxylation by Microsomal Fractions from Rat Livers and Yeast Cells Expressing Rat CYP2D2 or Human CYP2D6

| | $K_m$ ($\mu$M) | $V_{max}$ [a] | $K_i$ ($\mu$M) |
|---|---|---|---|
| Rat liver microsomes | | | |
| (A) Control | 1.6 | 2.73 | — |
| (B) Co-incubation[b] | 2.3 | 2.66 | 0.62 |
| (C) Preincubation[c] | 1.7 | 1.81 | 0.58 |
| Recombinant CYP2D2 | | | |
| (A) Control | 0.9 | 94.3 | — |
| (B) Co-incubation[b] | 1.7 | 95.8 | 0.33 |
| (C) Preincubation[c] | 0.9 | 42.5 | 0.25 |
| Recombinant CYP2D6 | | | |
| (A) Control | 3.6 | 16.7 | — |
| (B) Co-incubation[b] | 10.3 | 14.9 | 1.61 |
| (C) Preincubation[c] | 9.8 | 15.9 | 1.74 |

*a*) nmol/min/mg protein for rat liver microsomes; nmol/min/nmol CYP for recombinant enzymes. *b*) DMI (0.3 $\mu$M for the rat-derived enzymes; 3 $\mu$M for CYP2D6) together with BF (0.2 to 20 $\mu$M) was added to the equilibrated mixture and the mixture was incubated for 1 min. *c*) DMI (0.3 $\mu$M for the rat-derived enzymes; 3 $\mu$M for CYP2D6) was preincubated with the microsomal fraction in the presence of NADPH (0.5 M) at 37 °C for 2 min, followed by incubation with BF (0.2 to 20 $\mu$M) for 1 min. Each value is the mean of two independent determinations.

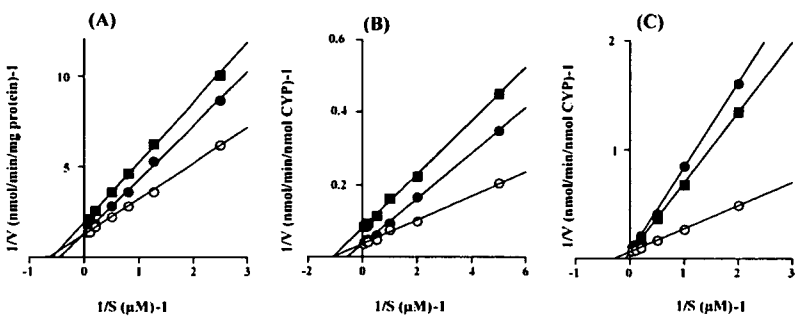


Fig. 3. Lineweaver-Burk Plots Showing the Inhibitory Effects of DMI on BF 1″-Hydroxyation by Rat Liver Microsomes and Yeast Cell Microsomes Expressing Rat CYP2D2 or Human CYP2D6

In the cases of rat liver microsomes (A) and CYP2D2 (B), DMI (0.3 $\mu$M) was used. In the case of human CYP2D6 (C), DMI (3.0 $\mu$M) was employed. Open circles, control; closed circles, co-incubation; closed squares, preincubation. The protocols for the co-incubation and preincubation are described in Chart 1. Each value represents the mean of duplicate determinations.

only CYP2D2 but also other enzyme(s) that function as BF 1″-hydroxylase and that are relatively resistant to the inactivation by DMI.

In the plots in Fig. 3C using human CYP2D6, on the other hand, the inhibition type was the same, *i.e.*, competitive inhibition, for both co-incubation and preincubation. Furthermore, the $K_i$ value calculated for the human recombinant enzyme was 1.7 $\mu$M, which was 5 to 6 times higher than that for the rat recombinant enzyme. This result supports the results in Fig. 2 showing that the inhibitory effect of DMI was much higher for BF 1″-hydroxylation by CYP2D2 than for that by CYP2D6.

**Inactivation of CYP2D2 by DMI** In order to further characterize the inactivation of CYP2D2 by DMI, the recombinant enzyme was preincubated with various concentrations of DMI in the presence of NADPH, and remaining enzyme activities were assayed. As shown in Fig. 4A, pseudo-first order kinetics were observed for the initial phase of the inactivation. Double reciprocal plots of the rate of inactivation of BF 1″-hydroxylase activity as a function of DMI concetration yielded $K_{inact}$ and $K_I$ values to be 0.19 $min^{-1}$ and 0.76 $\mu$M, respectively (Fig. 4B).

**Binding of DMI Metabolite(s) to CYP2D Enzymes** [$^3$H]-DMI (10 $\mu$M, 3600000 dpm) was incubated with yeast cell microsomal fractions expressing CYP2D2 or CYP2D6 (50 pmol) in the presence of an NADPH-generating system. After the incubation, a portion of the reaction mixture was subjected to SDS-PAGE. Proteins in the gels were transblotted to a PVDF membrane and were analyzed by Western blotting using polyclonal antibodies (rabbit IgG) raised against CYP2D1. In Fig. 5, the upper panels A and B are for CYP2D2 and the lower panels C and D for CYP2D6. In the Western blot analysis of CYP2D2 incubated with radioactive DMI (Fig. 5 panel A-b), there was only one protein band whose molecular weight was 51 kDa on the PVDF membrane. Imaging analysis of the membrane using the BAS2000 system showed that the 51 kDa protein was the only protein band with considerable radioactivity (Fig. 5, panel A-c).

The localization of radioactivity was also confirmed by cutting the slab gel after SDS-PAGE and measuring the radioactivity in the gel strips by liquid scintillation counting. As depicted in Fig. 5 panel B, there was a prominent radioactive peak whose location coincided with that of CYP2D2. On

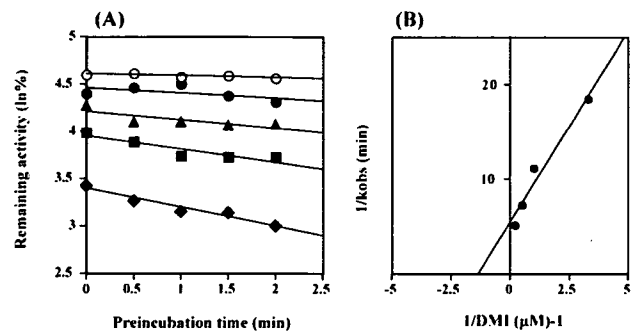


Fig. 4. Time- and Concentration-Dependent Loss of BF 1″-Hydroxylase Activity of CYP2D2 by Preincubation with DMI (A)

Incubation conditions were described under Materials and Methods. The concentrations of DMI were: open circles 0; closed circles 0.3 $\mu$M; closed triangles 1 $\mu$M; closed squares 2 $\mu$M; closed diamonds 5 $\mu$M. The reciprocal of first-order inactivation constants obtained from (A) and that of DMI concentrations were plotted (B), yielding the maximal rate of the inactivation ($K_{inact}$, 0.19 $min^{-1}$) and the inhibitor concentration required for the half-maximal rate of inactivation ($K_I$, 0.76 $\mu$M).

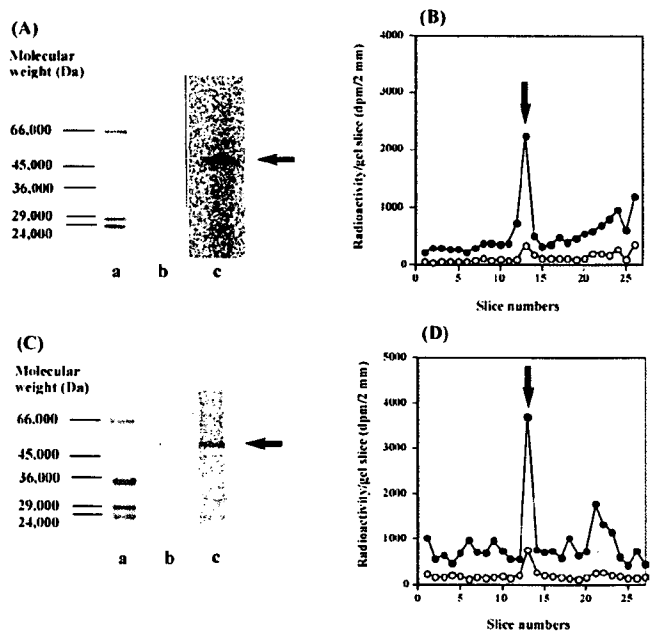


Fig. 5. Detection of Radioactive DMI Metabolite(s)-Bound Proteins by Western Blotting, BAS2000 Imaging Analysis and SDS-PAGE

The yeast cell microsomal fraction expressing rat CYP2D2 or human CYP2D6 (50 pmol each) was incubated with DMI under the conditions described in Materials and Methods. A part of the reaction medium was subjected to SDS-PAGE, and proteins in the gel were transblotted to a PVDF membrane. Proteins and their radioactivities were analyzed by Western blotting and using a BAS2000 image analyzer, respectively (left panels). Another part of the reaction medium was subjected to SDS-PAGE using a 10% slab-gel. The gel was cut into slices of 2 mm each, and their radioactivity was measured by liquid scintillation counting (right panels). Upper panels, rat CYP2D2; lower panels, human CYP2D6. The left panels: a, molecular weight markers; b, a PVDF membrane on which radiolabeled proteins were transblotted was analyzed by Western blotting; c, a scanning image of the PVDF membrane obtained using the BAS2000 imaging analyzer. The arrow shows the CYP2D proteins. The right panels: the sample was incubated in the presence (closed circles) or absence (open circles) of NADPH. Molecular weight markers; bovine albumin 66000; egg albumin, 45000; rabbit muscle glyceraldehyde 3-phosphate dehydrogenase, 36000; bovine carbonic anhydrase, 29000; bovine pancreas trypsinogen, 24000.

the basis of the radioactivity in the gel strip where CYP2D2 was localized, 33 pmol of radioactive metabolite(s) derived from DMI were calculated to bind to 50 pmol of CYP2D2. This means that DMI metabolite(s) were bound to about 70% of the enzyme during the incubation assuming that the binding mol ratio of the enzyme to the metabolite is 1. Results from the imaging analysis using the BAS2000 system also supported these conclusions (data not shown).

The results of binding experiments using human CYP2D6 were similar to those using rat CYP2D2 described above. In this case, 46 pmol of radioactive metabolite(s) derived from DMI were calculated to bind to 50 pmol of CYP2D6. However, in addition to the major peak of CYP2D6 protein, some radioactive peaks with molecular weights smaller than that of CYP2D6 were observed in Fig. 5 panel D, although they were not very prominent. BAS2000 imaging analysis also gave similar results (Fig. 5 panel C-c).

## DISCCUSSION

Our previous studies suggested that rat hepatic microsomal CYP2D enzyme(s) were inactivated by IMI during its oxidative metabolism.[8] In the present study, we confirmed that DMI also inhibited BF 1″-hydroxylation by recombinant CYP2D2 as well as by rat liver microsomes. However, CYP2D1, another major CYP2D enzyme in the rat liver, was not markedly affected by DMI under the conditions used.

Interestingly, BF 1″-hydroxylation by human liver microsomes was not affected by DMI at 0.3 $\mu$M, which efficiently inhibited the same reaction by rat liver microsomes and recombinant CYP2D2. The human liver microsmal preparations ($n$=3) used in this study were examined for their CYP2D6 contents (17.6±6.4 pmol/mg protein) and debrisoquine 4-hydroxylase activities (39.6±14.6 nmol/min/mg protein) prior to starting the present study. These results indicate that the functions of CYP2D6 in the human liver microsomal fractions used in the present study were within normal levels. Our finding that BF 1″-hydroxylation by recombinant CYP2D6 was not inhibited by DMI at 0.3 $\mu$M but was inhibited at 3.0 $\mu$M also suggests that the sensitivity of human CYP2D6 to DMI is lower than that of rat CYP2D2. The difference in the inhibition constants (0.3 $\mu$M for CYP2D2 and 1.7 $\mu$M for CYP2D6) well supports this notion.

In BF 1″-hydroxylation by the rat enzyme, the inhibition-type of DMI was found to change from competitive under the co-incubation conditions to noncompetitive under the preincubation conditions. To further characterize the inhibition properties, CYP2D2 was preincubated for 0.5 to 2 min with various concentrations of DMI in the presence of NADPH, followed by the assay of BF 1″-hydroxylase activity. The loss of the activity was found to be kinetically pseudo-first-order and saturable, indicating that DMI is a mechanism-based inhibitor for BF 1″-hydroxylation by CYP2D2.

From the profile of the change in the enzyme activity following co-incubation (Fig. 2b) and preincubation (Fig. 2c), the activity of the preincubated microsomes from yeast cell expressing CYP2D2 tends to be lower than that of the co-incubated microsomes (Figs. 2B, C). It is reasonable to think that competitive inhibition is responsible for the decreased activity in the co-incubation, whereas mechanism-based inactivation is mainly responsible for the decreased activity in the preincubation. In contrast, the activity of preincubated microsomes expressing CYP2D6 is higher than that of co-incubated microsomes. This result suggests that in this case, mechanism-based inactivation does not occur or if occurs, to much lesser extent as compared to the case of CYP2D2, and competitive inhibition is mainly responsible for the decreased activity of co-incubated and preincubated microsomes. The phenomenon that the activity of the preincubated microsomes was higher than that of the co-incubated microsomes may be due to the consumption to some extent of DMI during the preincubation with microsomes and the cofactor.

In another experiment using human CYP2D6, preincubation time was prolonged from 2 min to 4 or 6 min, yielding similar results in which the activities in the case of preincubation were higher than those in the case of co-incubation (data not shown). Therefore, it is feasible that, compared to rat CYP2D2, human CYP2D6 is resistant to the inactivation by DMI.

The binding study demonstrated that radioactivity derived from [$^3$H]-DMI bound to CYP2D2. Taking the results of the binding study into account, it is reasonable to think that some reactive metabolite(s) might be formed by CYP2D2 during the preincubation and bind to the enzyme, probably to an amino aid residue which is located in the active site of the enzyme, resulting in the inactivation of the enzyme.

It is noteworthy that in contrast to the results obtained with the rat enzyme, the human enzyme was not inactivated by preincubation with DMI and NADPH, though considerable radioactivity derived from [$^3$H]-DMI was shown to bind to the human enzyme. It is possible that, similarly to the case of the rat CYP2D2, some reactive metabolite(s) are formed from DMI by human CYP2D6 and bind to the enzyme. In this case, however, the binding of the metabolite(s) may not affect the function of the enzyme. It is unclear at present what species of reactive metabolite(s) of DMI and what amino acid residues of the enzymes are involved in the binding described above. Further studies proceeding in this laboratory will clarify these points in the near future.

In summary, the inhibitory effects of DMI on rat and human CYP2D enzymes were studied using BF 1″-hydroxylation as an index. BF 1″-hydroxylation was inhibited competitively when rat CYP2D2 was co-incubated with DMI and BF in the presence of NADPH and noncompetitively when the enzyme was preincubated with DMI and NADPH before the incubation with BF, whereas BF 1″-hydroxylation by rat CYP2D1 was not markedly affected under the same conditions. In contrast, BF 1″-hydroxylation by human liver microsomes and recombinant CYP2D6 was competitively inhibited by DMI in both the co-incubation and the preincubation. The loss of activity of rat CYP2D2 under the preincubation conditions followed pseudo-first-order kinetics. Binding experiments using the recombinant CYP2D enzymes revealed that CYP2D2 and CYP2D6 were the only prominent proteins to which considerable radioactive DMI metabolite(s) bound. These results indicate that DMI was metabolized by the CYP2D enzymes to reactive metabolite(s), which bind to CYP2D proteins, resulting in the inactivation of rat CYP2D2 but not human CYP2D6.

## REFERENCES


1) Sallee F. R., Pollock B. G., *Clin. Pharmacokinet.*, **18**, 346—364 (1990).
2) Koyama E., Chiba K., Tani M., Ishizaki T., *J. Pharmacol. Exp. Ther.*, **281**, 1199—1210 (1997).
3) Madsen H., Rasmussen B., Brosen K., *Clin. Pharmacol. Ther.*, **61**, 319—324 (1997).
4) Breyer U., *Naunyn-Schmiedebergs Arch. Pharmacol.*, **272**, 277—288 (1972).
5) Daniel W., Friebertshauser J., Steffen C., *Naunyn-Schmiedebergs Arch. Pharmacol.*, **328**, 83—86 (1984).
6) Daniel W., Netter J., *Naunyn-Schmiedebergs Arch. Pharmacol.*, **342**, 234—240 (1990).
7) Masubuchi Y., Takahashi C., Fujio N., Horie T., Suzuki T., Imaoka S., Funae Y., Narimatsu S., *Drug Metab. Dispos.*, **23**, 999—1003 (1995).
8) Masubuchi Y., Igarashi S., Suzuki T., Horie T., Narimatsu S., *J. Pharmacol. Exp. Ther.*, **279**, 724—731 (1996).
9) Wan J., Imaoka S., Chow T., Hiroi T., Yabusaki Y., Funae Y., *Arch. Biochem. Biophys.*, **348**, 383—390 (1997).
10) Omura T., Sato R., *J. Biol. Chem.*, **239**, 2370—2378 (1964).
11) Tsuzuki D., Takemi C., Yamamoto S., Tamagake K., Imaoka S., Funae Y., Kataoka H., Shinoda S., Narimatsu S., *Pharmacogenetics*, **11**, 709—718 (2001).
12) Narimatsu S., Imoto K., Isobe T., Kiryu K., Naito S., Hichiya H., Funae Y., Hanioka N., Yamamoto S., *Biochem. Biophys. Res. Commun.*, **324**, 627—633 (2004).
13) Yamaoka K., Tanigawara Y., Nakagawa T., Uno T., *J. Pharmacobio-Dyn.*, **4**, 879—885 (1981).
14) Silverman R. B., "Chemistry and Enzymology," Vol. 1, CRC Press, Boca Raton, FL, 1988, pp. 3—30.
15) Guengerich F. P., Wang P., Davidson N. K., *Biochemistry*, **21**, 1698—1706 (1982).
16) Lowry O. H., Rosebrough N. J., Farr A. L., Randall R. J., *J. Biol. Chem.*, **193**, 265—275 (1951).
17) Hiroi T., Imaoka S., Chow T., Funae Y., *Biochim. Biophys. Acta*, **1380**, 305—312 (1998).

# Four novel defective alleles and comprehensive haplotype analysis of *CYP2C9* in Japanese

Keiko Maekawa[a,b], Hiromi Fukushima-Uesaka[a], Masahiro Tohkin[a,c], Ryuichi Hasegawa[c], Hiroshi Kajio[d], Nobuaki Kuzuya[d], Kazuki Yasuda[e], Manabu Kawamoto[f], Naoyuki Kamatani[f], Kazuko Suzuki[g], Tatsuo Yanagawa[g], Yoshiro Saito[a,b] and Jun-ichi Sawada[a,b]

**Genetic variations in cytochrome P450 2C9 (*CYP2C9*) are known to contribute to interindividual and interethnic variability in response to clinical drugs such as warfarin. In the present study, *CYP2C9* from 263 Japanese subjects was resequenced, resulting in the discovery of 62 variations including 32 novel ones. In addition to the two known non-synonymous single nucleotide polymorphisms (SNPs), Ile359Leu (**3*; allele frequency=0.030) and Leu90Pro (**13*; 0.002), seven novel non-synonymous SNPs, Leu17Ile (0.002), Lys118ArgfsX9 (**25*; 0.002), Thr130Arg (**26*; 0.002), Arg150Leu (**27*; 0.004), Gln214Leu (**28*; 0.002), Pro279Thr (**29*; 0.002) and Ala477Thr (**30*; 0.002), were found. Functional characterization of novel alleles using a mammalian cell expression system *in vitro* revealed that **25* was a null allele and that **26*, **28* and **30* were defective alleles. The **26* product showed a 90% decrease in the $V_{max}$ value but little change in the $K_m$ value towards diclofenac. Both **28* and **30* products showed two-fold higher $K_m$ values and three-fold lower $V_{max}$ values than the **1* allele, suggesting the importance of Gln214 and Ala477 for substrate recognition. Linkage disequilibrium and haplotype analyses were performed using the detected variations. Only five haplotypes (frequency >0.02) accounted for most (>87%) of the inferred haplotypes, and they were closely associated with the haplotypes of *CYP2C19* in Japanese. Although the haplotype structure of *CYP2C9* was rather simple in Japanese, the haplotype distribution was quite different from those previously reported in Caucasians and Africans. Taken together, novel defective alleles and detailed haplotype structures would be useful for determining metabolic phenotypes of CYP2C9 substrate drugs in Japanese and probably Asians. *Pharmacogenetics and Genomics* 16:497–514 © 2006 Lippincott Williams & Wilkins.**

Pharmacogenetics and Genomics 2006, 16:497–514

Keywords: ***CYP2C9*, function, haplotype, Japanese, non-synonymous SNP**

[a]Project Team for Pharmacogenetics, [b]Division of Biochemistry and Immunochemistry, [c]Division of Medicinal Safety Science, National Institute of Health Sciences, Tokyo, Japan, [d]Division of Endocrine and Metabolic Diseases, the Hospital, [e]Department of Metabolic Disorder, Research Institute, International Medical Centre of Japan, Tokyo, Japan, [f]Division of Genomic Medicine, Department of Advanced Biomedical Engineering and Science, Tokyo Women's Medical University, Tokyo, Japan and [g]Nerima General Hospital, Tokyo, Japan.

Correspondence and requests for reprints to Keiko Maekawa, Division of Biochemistry and Immunochemistry, National Institute of Health Sciences, 1-18-1 Kamiyoga, Setagaya-ku, Tokyo 158-8501, Japan.
Tel: +81 3 3700 9453; fax: +81 3 5717 3832;
e-mail: maekawa@nihs.go.jp

Sponsorship: This study was supported in part by the Program for the Promotion of Fundamental Studies in Health Sciences, by the Health and Labour Sciences Research Grant (Research on Advanced Medical Technology) from the Ministry of Health, Labour and Welfare.

Received 29 December 2005 Accepted 22 February 2006

## Introduction

Cytochrome P450 2C9 (CYP2C9) is said to metabolize approximately 15% of the drugs that undergo Phase I metabolism. This enzyme belongs to the human CYP2C subfamily (including CYP2C8, CYP2C9, CYP2C18 and CYP2C19) and hydroxylates weakly acidic or neutral drugs of diverse therapeutic categories, including the hypoglycemic agents tolbutamide and glimepiride, the anticonvulsant phenytoin, the anticoagulant warfarin, the non-steroidal anti-inflammatory drugs flurbiprofen and diclofenac, the antihypertensive losartan, and the diuretic torsemide [1]. Several genetic polymorphisms in *CYP2C9* are already known to affect the metabolism of many of these drugs [2]. However, highly variable interindividual and ethnic differences in the metabolisms of these CYP2C9 substrate drugs [3,4] suggest that the unidentified genetic, dietary, or ethnic-specific environmental factors might account for these differences.

To date, at least 24 non-synonymous *CYP2C9* alleles have been identified and published on the Human CYP Allele Nomenclature Committee homepage (http://www.imm.ki.se/CYPalleles/). The **2* (Arg144Cys) and **3* (Ile359Leu) alleles of *CYP2C9* are found in Caucasians at frequencies of 10–15% and 5–10%, respectively, but are less prevalent in African-American and Asian populations, and exhibit reduced activities towards a number of substrates such as warfarin, phenytoin and losartan both *in vitro* and *in vivo* [5]. In particular, the subjects bearing the diplotype, **2/*3* or **3/*3*, showed lowered daily warfarin or phenytoin dose

1744-6872 

requirements and appeared to be more susceptible to their adverse effects during initiation of therapy [6]. On the other hand, a number of reported alleles (**4* to **24*), some of which exhibit catalytic defects, are mostly ethnic-specific and relatively rare [7–13].

It is possible that the single nucleotide polymorphisms (SNPs) in the promoter region of *CYP2C9* are responsible for altering metabolic activities, which may result in adverse reactions or therapeutic failures. These SNPs might influence not only the basal transcriptional activity, but also the induction of *CYP2C9* by various drugs such as rifampicin and phenobarbital [14]. A previous study in a Japanese population indicated that promoter SNPs of *CYP2C9* were associated with reduced intrinsic clearance of phenytoin, but these findings might be due largely to the linkage between the **3* allele and promoter SNPs (−1911T > C, −1885C > G, −1537G > A and −981G > A) [15]. Other studies on Caucasian, Asians and Japanese did not find any associations between the promoter SNPs and warfarin sensitivity [12,13,16,17] or acenocoumarol pharmacodynamics [18].

Collectively, the known genetic variations in *CYP2C9* can only partially explain the interindividual or ethnic differences in CYP2C9 activity *in vivo*. A recent extensive review on allelic variants of 11 Phase I enzyme genes has pointed out that members of the CYP2 subfamily have the highest level of genetic diversity [19]. Very recently, Ahmadi *et al.* [20] illustrated differences in long-range linkage disequilibrium (LD) profiles of the CYP2C cluster covering the four *CYP2C* genes (*2C18*, *2C19*, *2C8* and *2C9*) between Europeans and Japanese. These reports have prompted us to resequence *CYP2C9* in Japanese and to identify detailed Japanese-specific genetic variations and haplotype structures.

In the present study, we sequenced the coding exons, their flanking introns and the upstream putative promoter regions in *CYP2C9* from 263 Japanese subjects. Seven novel alleles with non-synonymous SNPs were functionally assessed by using diclofenac as a substrate in a mammalian cell expression system. In addition, the haplotype structures with high-density SNPs were analysed and compared with those in previous reports to provide a plausible explanation for the variability in the in-vivo metabolic activity of CYP2C9 in different ethnic groups. Furthermore, the associations between *CYP2C9* and *CYP2C19* haplotypes in Japanese were analysed.

## Materials and methods

### Human genomic DNA samples

Two hundred and sixty-three Japanese subjects analysed in this study consisted of 134 diabetic patients and 129 healthy volunteers. The diabetic patients were administered an antidiabetic drug, glimepiride, at the International Medical Center of Japan or Nerima General Hospital. Healthy volunteers were recruited at Tokyo Women's Medical University. Genomic DNA was extracted from blood leukocytes of diabetic patients and from Epstein–Barr virus-transformed lymphoblastoid cells derived from healthy volunteers. Written informed consent was obtained from all participating subjects. The ethical review boards of the International Medical Center of Japan, the Nerima General Hospital, the Tokyo Women's Medical University, and the National Institute of Health Sciences approved this study.

### Polymerase chain reaction (PCR) conditions for DNA sequencing

First, multiplex PCR was performed to amplify the 5′-flanking region or all nine exons of *CYP2C9* by using the two sets of mixed primers (Mix 1 and Mix 2 in 'first PCR', respectively, as listed in Table 1). Namely, the four (5′-flanking, exons 2–3, 6 and 7) or three (5′-flanking to exon 1, exons 4–5 and 8–9) genomic DNA fragments were amplified simultaneously from 50 ng of genomic DNA using 1.25 U of Ex-Taq (Takara Bio. Inc., Shiga, Japan) with 0.60 μM mixed primers. The first PCR conditions were 94°C for 5 min, followed by 30 cycles of 94°C for 30 s, 55°C for 1 min and 72°C for 2 min; and then a final extension for 7 min at 72°C. Next, the 5′-flanking region and each exon were amplified separately (second PCR) using the first PCR products as template with Ex-Taq (1.25 U) and the primer sets (0.4 μM); listed in the 'second PCR' of Table 1. To cover approximately 3 kb from the transcriptional initiation site, three discontinuous fragments of the 5′-flanking region (−3377 to −2590, −2093 to −1506 and −1283 to −106) were amplified by second PCR. The regions −2589 to −2094 and −1505 to −1284 were omitted from the present analysis. For the amplification of each exon, the flanking intronic sites were included to analyse the sequences of exon–intron splice junctions. The second PCR conditions were the same as the first PCR. The PCR products were then treated with a PCR Product Pre-Sequencing Kit (USB Co., Cleveland, Ohio, USA) and sequenced directly on both strands using an ABI BigDye Terminator Cycle Sequencing Kit (Applied Biosystems, Foster City, California, USA) with the primers listed in 'sequencing' of Table 1. The excess dye was removed by a DyeEx96 kit (Qiagen, Hilden, Germany). The eluates were analysed on an ABI Prism 3730XL DNA Analyser (Applied Biosystems). All the novel SNPs were confirmed by repeated sequencing of the PCR products generated by new genomic DNA amplifications. The genomic and cDNA sequences of *CYP2C9* obtained from GenBank (NT_030059.12 and NM_000771.2, respectively) were used as the reference sequences. Description of SNPs was based on the cDNA sequence, and adenine of the translational initiation site in exon 1 was numbered + 1.

### Cloning and site-directed mutagenesis of CYP2C9 cDNA

Construction of the wild-type CYP2C9 expression plasmid (pcDNA3.1D/CYP2C9/wild-type) was performed

**Table 1** Primer sequences used for the analysis of the human *CYP2C9* gene

| Amplified and sequenced region | | | Forward primer | | Reverse primer | | |
|---|---|---|---|---|---|---|---|
| | | | Sequence (5′ to 3′) | Position[b] | Sequence (5′ to 3′) | Position[b] | PCR product (bp) |
| First PCR | Mix 1 | 5′-flanking (−4658 to −1506)[a] | CTATGAAGCTAATCAAGACAGTGTGC | 15442308 | CTCATGTCCCTTTTGAATCTCT | 15445460 | 3153 |
| | | Exons 2–3 | GTAGAGACGTGGTATCACCTTG | 15449746 | GGTAATGGGAAAAACACTGCT | 15450959 | 1214 |
| | | Exon 6 | AAGAGCCTGATGAATGGAAT | 15480157 | ACTACAGATGGGATTTGGC | 15480811 | 655 |
| | | Exon 7 | GACTTACCCATGCCCCTTTG | 15489144 | ATCTGGAGAACACACACTGC | 15489858 | 715 |
| | Mix 2 | 5′-flanking to exon 1 (−1702 to exon 1)[a] | CCAACTGAACTGAATGTTTTGC | 15445264 | GAATCTAACATGCAAAGACCC | 15447354 | 2091 |
| | | Exons 4–5 | TTGGTTCCTCTCTACTGGTTC | 15455622 | GGTAGTTTATATTTCTGTGGGCTC | 15457823 | 2202 |
| | | Exons 8–9 | GTTGCATCCAAGTATCCAAG | 15494067 | CTCTAACACTCACCCAAAATAGC | 15497828 | 3762 |
| Second PCR | | 5′-flanking (−3377 to −2590)[a] | ATCTGGTAGTTGTGCTCTTTGG | 15443589 | CATGTCACATCCCATCTCATAG | 15444376 | 788 |
| | | 5′-flanking (−2093 to −1506)[a] | TAAACTGAAAGGTCTAGGAAGG | 15444873 | CTCATGTCCCTTTTGAATCTCT | 15445460 | 588 |
| | | 5′-flanking (−1283 to −106)[a] | ATCCTCAACTCAGTATGTCAGC | 15445683 | ATCACCTAGGTCCACTATATGC | 15446860 | 1178 |
| | | Exon 1 (−245 to exon 1)[a] | CTCCAACCAAGTACAGTGAA | 15446721 | GAATCTAACATGCAAAGACCC | 15447354 | 634 |
| | | Exons 2–3 | GTAGAGACGTGGTATCACCTTG | 15449746 | GGTAATGGGAAAAACACTGCT | 15450959 | 1214 |
| | | Exon 4 | TTGGTTCCTCTCTACTGGTTC | 15455622 | GCAGAAAAAACATTGATGAGGGAG | 15456464 | 843 |
| | | Exon 5 | CTGGTTAGAATTGATCCTCTG | 15457180 | GGTAGTTTATATTTCTGTGGGCTC | 15457823 | 644 |
| | | Exon 6 | AAGAGCCTGATGAATGGAAT | 15480157 | ACTACAGATGGGATTTGGC | 15480811 | 655 |
| | | Exon 7 | GACTTACCCATGCCCCTTTG | 15489144 | ATCTGGAGAACACACACTGC | 15489858 | 715 |
| | | Exon 8 | GTTGCATCCAAGTATCCAAG | 15494067 | CCAACCTATATTTCAGCTTTCTC | 15494695 | 629 |
| | | Exon 9 | CTCATCCATCCATTCATTCATG | 15496956 | CTCTAACACTCACCCAAAATAGC | 15497828 | 873 |
| Sequencing | | 5′-flanking (−3373 to −2590)[a] | GGTAGTTGTGCTCTTTGGTA | 15443593 | CATGTCACATCCCATCTCATAG | 15444376 | |
| | | 5′-flanking (−2093 to −1506)[a] | TAAACTGAAAGGTCTAGGAAGG | 15444873 | CTCATGTCCCTTTTGAATCTCT | 15445460 | |
| | | 5′-flanking (−1283 to −612)[a] | ATCCTCAACTCAGTATGTCAGC | 15445683 | ACCTTTACCATTAAACCCCC | 15446354 | |
| | | 5′-flanking (−659 to −137)[a] | CAATTCCTGCCTTCAGGA | 15446307 | AAGGACTTTGACCCACTGAT | 15446829 | |
| | | Exon 1 (−222 to exon 1)[a] | GGAATGTACAGAGTGGACAATG | 15446744 | GACCCAAATCTTTCTCTACT | 15447338 | |
| | | Exon 2 | TCTTGAACTCCTGACCTTGT | 15449781 | GGAGCTCTGTAAGTCTCTGT | 15450378 | |
| | | Exon 3 | AGGAGTTTTCTGGAAGAGG | 15450247 | GGAAAAACACTGCTCTTTAACTC | 15450952 | |
| | | Exon 4 | CCTTTCCATCTCAGTGCCTT | 15455707 | GCCGTCTTTCCCAGATATTC | 15456374 | |
| | | Exon 5 | CTGGTTAGAATTGATCCTCTG | 15457180 | GGTAGTTTATATTTCTGTGGGCTC | 15457823 | |
| | | Exon 6 | GCATGGAATAAGGGAGTAGG | 15480187 | ACTACAGATGGGATTTGGC | 15480811 | |
| | | Exon 7 | CCATGCCCCTTTGTTATTTG | 15489151 | AACACACACTGCCAGACACTAG | 15489850 | |
| | | Exon 8 | GTTGCATCCAAGTATCCAAG | 15494067 | CCAACCTATATTTCAGCTTTCTC | 15494695 | |
| | | Exon 9 | CTCATCCATCCATTCATTCATG | 15496956 | CGAATGTTCACTAGATCTTCAG | 15497455 | |
| | | Exon 9 | CTGCAGCTCTCTTTCCTC | 15497348 | CTCTAACACTCACCCAAAATAGC | 15497828 | |

[a]A of the translational start codon is 1, based on NT_030059.12.
[b]The nucleotide position of the 5′ end of each primer on NT_030059.12. PCR, Polymerase chain reaction.

using pcDNA3.1 Directional TOPO Expression kit (Invitrogen, Carlsbad, California, USA). Briefly, the wild-type CYP2C9 cDNA was amplified by PCR from human adult normal liver Quick-Clone cDNA (Clontech, Palo Alto, California, USA) with the forward primer, 5′-*CACC*AGAAGGCTTCAATGGATTCTC-3′, and the reverse primer, 5′-GAGAAAAGGCATTACAGATAGTG-3′. The sequence in italics was introduced for the directional TOPO cloning system. The PCR products were cloned directly into the pcDNA3.1D/TOPO vector according to the manufacturer's instructions. Seven single CYP2C9 variations, 49C > A (Leu17Ile), 353_362del AGAAATGGAA (Lys118ArgfsX9, which denotes a frame shift starting with Lys118Arg and ending with a stop codon at the 9th residue), 389C > G (Thr130Arg), 449G > T (Arg150Leu), 641A > T (Gln214Leu), 835C > A (Pro279Thr) and 1429G > A (Ala477Thr), were introduced into the wild-type plasmid (pcDNA3.1D/CYP2C9/Wild-type) using a QuickChange Site-Directed Mutagenesis Kit (Stratagene, La Jolla, California, USA). The primer sequences used for the construction of variant plasmids were: 5′-GTCTCTCAT GTTTGCTTCTC***A***TTTCACTCTGGAGACAGAGC-3′ (sense) and 5′-GCTCTGTCTCCAGAGTGAAA***T***GAGA AGCAAACATGAGAGAC-3′ (antisense) for pcDNA3.1D/CYP2C9/Leu17Ile, 5′- GAATTGTTTTCAGCAATGGA A^GGAGATCCGGCGTTTCT-3′ (sense) and 5′-AGAA ACGCCGGATCTCC^TTCCATTGCTGAAAACAATT C-3′ (antisense) for pcDNA3.1D/CYP2C9/Lys118ArgfsX9, 5′-CGTTTCTCCCTCATGA***G***GCTGCGGAATTTTGG G-3′ (sense) and 5′-CCCAAAATTCCGCAGC***C***TCATGA GGGAGAAACG-3′ (antisense) for pcDNA3.1D/CYP2C9/Thr130Arg, 5′-TCAAGAGGAAGCCC***T***CTGCCTTGTG GAGG-3′ (sense) and 5′-CCTCCACAAGGCAG***A***GGGC TTCCTCTTGA-3′ (antisense) for pcDNA3.1D/CYP2C9/Arg150Leu, 5′-GCAGCCCCTGGATCC***T***GATCTGCAA TAATTTTTCT-3′ (sense) and 5′-AGAAAAATTATTG CAGATC***A***GGATCCAGGGGCTGC-3′ (antisense) for pcDNA3.1D/CYP2C9/Gln214Leu, 5′-GAGAAGGAAAAG CACAACCAA***A***CATCTGAATTTACTATTGAAAGCTT-3′ (sense) and 5′-AAGCTTTCAATAGTAAATTCAGATG***T***T TGGTTGTGCTTTTCCTTCTC-3′ (antisense) for pcDNA3.1D/CYP2C9/Pro279Thr, 5′-CAGTTGTCAATG GATTT***A***CCTCTGTGCCGCCCT-3′ (sense) and 5′-AGG GCGGCACAGAGG***T***AAATCCATTGACAACTG-3′ (antisense) for pcDNA3.1D/CYP2C9/Ala477Thr. The positions where the nucleotides are exchanged or deleted are in italic and bold or indicated with the mark ^, respectively. To ensure that no errors had been introduced during amplification, the entire cDNA regions were confirmed by sequencing all plasmid constructs.

### Transient transfection in COS-1 cells and preparation of microsomal fractions

COS-1 cells, an African green monkey kidney cell line, were cultured in Dulbecco's Modified Eagle's Medium (DMEM) with 100 U/ml penicillin, 0.1 mg/ml streptomycin and 10% fetal bovine serum under 5% $CO_2$ at 37°C. The cells ($2.4 \times 10^6$) were seeded in a 10-cm culture dish one day before transfection. After 24 h of culture, the cells were rinsed with serum-free DMEM. Fourteen μg of the wild-type or variant CYP2C9 or empty pcDNA3.1 plasmid was transfected using the LIPOFECTAMINE 2000 reagent (Invitrogen) according to the manufacturer's instructions. After 28 h after transfection, the cells were rinsed with ice-cold 10 mM phosphate buffered saline (pH 7.4) and scraped in 50 mM potassium phosphate buffer (pH 7.4) containing 0.25 M sucrose, 25 mM KCl and 0.5 mM ethylenediamine tetraacetic acid. Microsomes from transfected COS-1 cells were prepared by sequential centrifugation according to a standard procedure described by Ekins *et al.* [21]. After centrifugation, the microsomes were suspended in 100 mM potassium phosphate buffer (pH 7.4) and stored at −90°C until used. The protein concentration of the microsomes was assayed with the Protein Assay Kit (BioRad Lab., Hercules, California, USA) using bovine γ globulin as a standard.

### Determination of CYP2C9 mRNA expression levels by TaqMan real-time reverse transcription (RT)-PCR

Total cellular RNA was isolated from the transfected COS-1 cells using the RNAeasy Mini kit (Qiagen), and then treated with RNase-free DNase (Invitrogen) to avoid plasmid DNA contamination in the samples. DNase-treated total RNA (500 ng) was used to prepare first-strand cDNA with a High-Capacity cDNA Archive kit (Applied Biosystems) using random primers. Real-time PCR assays were performed by an ABI PRISM 7700 Sequence Detection System using TaqMan Gene Expression Assay for CYP2C9 (Assay ID: Hs01682803_mH, Applied Biosystems) according to the manufacturer's recommendations. The TaqMan probe used for this assay was designed to bind to the junction between exons 1 and 2 of human CYP2C9 cDNA.For internal controls, β-actin mRNA levels were quantified using TaqMan β-actin control reagents (Applied Biosystems). Standard curves of CYP2C9 and β-actin were obtained from a serial dilution of cDNAs from COS-1 cells expressing wild-type CYP2C9. For each sample, the relative amount of mRNA of the target (CYP2C9) and the control (β-actin) were determined, and the CYP2C9 mRNA expression level was normalized against β-actin mRNA levels and expressed as a ratio to the wild-type (100%). Expression levels were shown as mean ± SD of four to six separate transfection experiments.

### Determination of protein expression levels by immunoblotting

Western blotting was performed to determine the protein expression levels of CYP2C9 and calnexin, an endoplasmic reticulum-resident protein, as a control. Thirty μg protein of the microsomal fractions from COS-1 cells were dissolved in sodium dodecyl sulfate (SDS)-sample

buffer, separated by electrophoresis in 8% SDS-polyacrylamide gels, and transferred onto nitrocellulose membranes (Schleicher & Schuell Inc., Dassel, Germany). For immunostaining of CYP2C9, goat anti-CYP2C6 antiserum (diluted 1:1000, Daiichi Pure Chemical Co., Tokyo, Japan), which can cross-react with human CYP2C9, and horseradish peroxidase-conjugated rabbit anti-goat IgG (diluted 1:20,000, Jackson ImmunoResearch Laboratories, West Grove, Pennsylvania, USA) were used as the first and second antibodies, respectively. Calnexin was detected with rabbit anti-calnexin antiserum (diluted 1:2000, StressGen Biotechnologies Corp., Victoria, British Columbia, Canada) and donkey anti-rabbit IgG (diluted 1:4000, GE Healthcare, Piscataway, New Jersey, USA). Immunoreactive proteins were visualized with Western Lightning Chemiluminescence Reagent Plus (PerkinElmer Life Sciences, Boston, Massachusetts, USA), and the band densities were quantified with Diana III and Zero Dscan software (Raytest, Straubenhardt, Germany). Commercially available microsomes of human CYP2C9-expressing lymphoblast cells (BD Gentest, Woburn, Massachusetts, USA) were used as a calibration standard. Quantification was performed within a linear range of its fluorescent intensity. CYP2C9 levels from three independent transfection experiments were determined based on mg of microsomal protein, which was normalized to calnexin content.

**Assay for CYP2C9-mediated enzymatic activity**

CYP2C9 activities for the wild-type and seven variants were assessed by diclofenac 4′-hydroxylation according to the method of Leemann *et al.* [22] with some modifications. Diclofenac and 4′-hydroxydiclofenac were purchased from Sigma (St Louis, Missouri, USA) and BD Gentest, respectively. The incubation mixture contained diclofenac (2.5–100 μM), the microsomal fraction (400 μg protein) from COS-1 cells, human NADPH-P450 Reductase microsomes (150 μg protein, BD Gentest), a NADPH regenerating system (1.3 mM $NADP^+$, 3.3 mM glucose 6-phosphate, 3.3 mM $MgCl_2 \cdot 6H_2O$, and 0.4 U/ml glucose-6-phosphate dehydrogenase), and 100 mM Tris-HCl buffer (pH 7.5) in a final volume of 500 μl. Diclofenac was dissolved in methanol [final concentration of methanol in reaction medium was 1% (v/v)]. After preincubation at 37°C for 5 min, the reaction was started by the addition of microsomes and allowed to proceed at 37°C for 50 min. The reaction was stopped on ice by the addition of 100 μl of 96% acetonitrile acidified with 4% glacial acetic acid. The samples were then subjected to centrifugation at 6000*g* for 20 min at 4°C, and the resulting supernatants were filtered through 0.2 mM pore size polytetra-fluoroethylene membrane filters (Millipore, Bedford, Massachusetts, USA). The formation of the metabolite 4′-hydroxydiclofenac was linear under our conditions up to 50 min. Preliminary experiments also showed that the amount of exogenous NADPH-P450 reductase microsome (150 μg protein), which was equivalent to 0.345 U, was sufficient to support the optimum activity of CYP2C9 expressed in COS-1 cells.

The production of 4′-hydroxydiclofenac was determined by reverse-phase high-performance liquid chromatography (HPLC). HPLC analysis was performed using a JASCO GULLIVER system consisting of PU-980 pumps, UV-970 detector, AS-2057Plus autosampler, and CO-2065Plus column oven, which were all controlled by JASCO-BORWIN/HSS-2000 programs (Nihon Bunko, Tokyo, Japan). Aliquots of the supernatants (100 μl) were injected into an Inertsil ODS-3 column (5 μm, 250 × 4.6 mm i.d., GL Sciences, Tokyo, Japan) connected to a pre-column (GL Sciences). The mobile phase consisted of 30% acetonitrile containing 1 mM perchloric acid (A) and methanol (B), forming a 20-min linear gradient from 30% to 100% of B at a flow rate of 1 ml/min. The ultraviolet wavelength was fixed at 280 nm, and the column was maintained at 50°C. Under these conditions, the retention times of 4′-hydroxydiclofenac and diclofenac were 11 and 15 min, respectively. The standard curve was obtained within the range from 1.25 μM to 10.0 μM for 4′-hydroxydiclofenac. The detection limit of the metabolite was 10 pmol, which corresponded to the enzyme activity of 3.0 pmol/min/mg protein. The interday variation coefficients of diclofenac 4′-hydroxylation assay did not exceed 6% ($n = 4$). Kinetic parameters such as $K_m$ and $V_{max}$ were estimated using the computer program designed for non-linear regression analysis of a hyperbolic Michaelis–Menten equation (Prism v.3.0a, GraphPad Software, San Diego, California, USA). Data are presented as the mean ± SD for three microsomal preparations derived from separate transfections for each variant and analysed by one-way analysis of variance, and multiple comparisons were made with the Scheffe test.

**Linkage disequilibrium (LD) and haplotype analysis**

Hardy–Weinberg equilibrium and LD analysis was performed by SNPAlyse software (Dynacom Co., Yokohama, Japan), and a pairwise LD between variations was obtained for $|D'|$ and rho square ($r^2$) values. Some of the haplotypes were unambiguous from subjects with homozygous variations at all sites or a heterozygous variation at only one site. The diplotype configurations were inferred by LDSUPPORT software, which determines the posterior probability distribution of the diplotype for each subject based on the estimated haplotype frequencies [23]. We designated the haplotypes as follows: the group of haplotypes without amino acid changes was defined as **1*, and the groups with amino acid changes (Ile359Leu and Leu90Pro) were numbered (**3* and **13*, respectively) according to the designations by the Human Cytochrome P450 (CYP) Allele Nomenclature Committee. Six newly identified haplotypes (alleles) with novel non-synonymous variations (*CYP2C9*25* to **30*) have been registered to the Human Cytochrome P450 (CYP) Allele

Nomenclature Committee. Subtypes within each haplotype group were consecutively named with small alphabetical letters depending on their frequencies, except for **1A*, **1B* and **3B*, which were already assigned by the Committee. We could not detect the **1C* and **1D* haplotypes in our study. To avoid confusion with the nomenclature by the CYP Allele Nomenclature Committee, other **1* haplotypes were tentatively named (**1e* to **1al*). The haplotypes inferred in only one chromosome are shown as the haplotype name plus a question mark, since the predictability for these very rare haplotypes is known to be low in some cases.

Network analysis of unambiguous haplotypes was performed with Network 4.1.0.9 (www.fluxus-engineering.com) based on the algorithms of the reduced median network. The long-range haplotypes spanning *CYP2C19* and *CYP2C9* were inferred by Hapblock software (www.cmb.usc.edu/msms/HapBlock/).

## Results

### *CYP2C9* variations found in a Japanese population

We found 62 variations including 32 novel ones by analysing the promoter regions, all nine exons and their flanking regions of *CYP2C9* from 263 Japanese subjects (Table 2). The distribution of the variations included 18 in the 5′ flanking region, 14 (five synonymous and nine non-synonymous) in the coding exons, 27 in the introns, two in the 3′-untranslated region (3′-UTR), and one in the 3′-flanking region. All of the detected variations were in Hardy–Weinberg equilibrium for two separate groups ($P \geq 0.37$ in diabetic patients and $P \geq 0.20$ in healthy volunteers) and for all subjects ($P \geq 0.44$). Since we did not find any significant differences in the frequencies between the healthy volunteers and diabetic patients ($P > 0.05$ by $\chi^2$ test or Fisher's exact test), the data for all subjects were analysed as one group.

Ten novel variations were identified in the coding region, of which three, 336T > C (Ile112Ile), 798C > T (Cys266Cys) and 1137T > C (Tyr379Tyr), were synonymous, and seven, 49C > A (Leu17Ile), 353_362del AGAAATGGAA (Lys118ArgfsX9), 389C > G (Thr130Arg), 449G > T (Arg150Leu), 641A > T (Gln214Leu), 835C > A (Pro279Thr) and 1429G > A (Ala477Thr), were non-synonymous. All the non-synonymous variations were found as single heterozygotes (allele frequencies = 0.002), except for 449G > T (Arg150Leu), which was present in two subjects (frequency = 0.004). The six novel alleles were designated as **25* (Lys118ArgfsX9), **26* (Thr130Arg), **27* (Arg150Leu), **28* (Gln214Leu), **29* (Pro279Thr) and **30* (Ala477Thr) by the Human Cytochrome P450 Allele Nomenclature Committee. Another novel allele, 49C > A (Leu17Ile), was tentatively named **17I* because the subject carrying this allele was heterozygous also for **3* (1075A > C, Ile359Leu).

In the 5′ flanking region, nine novel SNPs (−3279T > C, −3070G > A, −2980C > T, −2787G > T, −2718G > A, −2711C > T, −1924A > G, −885A > G and −732T > G) were detected at an allele frequency of 0.002. Recent studies on functional nuclear receptor binding sites in the promoter region in *CYP2C9* revealed two constitutive androstane receptor-responsive elements (CAR-REs) between positions −2900 and −2841 [24] and between −1839 and −1824 [25] from the translation initiation site, one glucocorticoid receptor-responsive element (GRE) between −1697 and −1683 [25] and two proximal HNF4α binding sites between −152 and −129 and between −185 and −163 [14,26]. However, novel SNPs were not found in these established elements.

The remaining 13 novel variations were found either in the intronic region or 3′-UTR with allele frequencies less than 0.01. These variations seem unlikely to affect splicing because they were not located in the exon-intron splicing junctions or branch sites.

Thirty variations were already reported or publicized in the dbSNP database and/or the Human Cytochrome P450 Allele Nomenclature Committee homepage. Their ID numbers in the databases and references are provided in Table 2. We found two reported non-synonymous SNPs, 269T > C (**13*, Leu90Pro) and 1075A > C (**3*, Ile359Leu), at allele frequencies of 0.002 and 0.03, respectively. However, 430C > T (**2*, Arg144Cys) was not found in our Japanese population. As for the promoter SNPs, the substitution −2875C > G, located within distal CAR-RE (−2900 to −2841), was found [24]. The relatively frequent SNPs −3089G > A, −2665_−2664delTG, −1565C > T and −1188T > C were also detected.

### Expression levels of the seven CYP2C9 variants

To functionally characterize the non-synonymous variations, the wild-type and each of the seven variant proteins (Leu17Ile, Lys118ArgfsX9, Thr130Arg, Arg150Leu, Gln214Leu, Pro279Thr and Ala477Thr) were transiently expressed in transfected COS-1 cells. First, expression levels of CYP2C9 proteins were assessed by Western blotting. Representative data obtained from three independent transfections are shown in Fig. 1. Expression levels of the endoplasmic reticulum-resident protein, calnexin, were almost constant in microsomes from the transfected cells. No CYP2C9 protein expression was detected, even as proteolytic fragments, for the Lys118ArgfsX9 variant (The residues 118–126, Lys-Lys-Trp-Lys-Glu-Ile-Arg-Arg-Phe, were changed to Arg-Arg-Ser-Gly-Val-Ser-Pro-Ser-Stop.) and the empty vector (Fig. 1a, b). The expression level of wild-type CYP2C9 was calculated as 12.0 ± 2.5 pmol/mg microsomal protein. No significant differences were shown in the expression levels of CYP2C9 protein among the wild-type and the other six variants ($P = 0.84$, Fig. 1b).

**Table 2** Summary of *CYP2C9* single nucleotide polymorphisms detected in a Japanese population

| Location | Position | | Nucleotide change and flanking sequences (5′–3′) | Amino acid change | Number of subjects | | | Allele Frequency | dbSNP SNP ID (NCBI) | Reference[c] |
|---|---|---|---|---|---|---|---|---|---|---|
| | NT_030059.12 | From the translational initiation site or from the end of nearest exon | | | Wild-type | Heterozygote | Homozygote | | | |
| 5′-Flanking | 15443687 | −3279[a] | CATCA**T**/CTGTCA | | 262 | 1 | 0 | 0.002 | | |
| 5′-Flanking | 15443877 | −3089 | CAACCG/**A**TATTA | | 134 | 106 | 23 | 0.289 | rs12782374 | |
| 5′-Flanking | 15443896 | −3070[a] | AAAAGG/**A**CAAAA | | 262 | 1 | 0 | 0.002 | | |
| 5′-Flanking | 15443986 | −2980[a] | TAGGGC/**T**AGTAA | | 262 | 1 | 0 | 0.002 | | |
| 5′-Flanking | 15444091 | −2875 | ATGAGC/GTTTGG | | 262 | 1 | 0 | 0.002 | | [10] |
| 5′-Flanking | 15444179 | −2787[a] | GTGCAG/**T**GGAAA | | 262 | 1 | 0 | 0.002 | | |
| 5′-Flanking | 15444248 | −2716[a] | CAAAAG/ACCTAC | | 262 | 1 | 0 | 0.002 | | |
| 5′-Flanking | 15444255 | −2711[a] | CTACTC/**T**TAATC | | 262 | 1 | 0 | 0.002 | | |
| 5′-Flanking | 15444301_15444302 | −2665_−2664 | GTGAC**T**G/−TGGAG | | 134 | 106 | 23 | 0.289 | | [13,16] |
| 5′-Flanking | 15445042 | −1924[a] | GAGTCA/GGGGAC | | 262 | 1 | 0 | 0.002 | | |
| 5′-Flanking | 15445055 | −1911 | AGTTA**T**/CTGCTT | | 247 | 16 | 0 | 0.030 | rs9332092 | |
| 5′-Flanking | 15445081 | −1885 | AAAGGC/GTTCTC | | 247 | 16 | 0 | 0.030 | rs9332093 | |
| 5′-Flanking | 15445401 | −1565 | CATTCC/**T**GGAAA | | 202 | 56 | 5 | 0.125 | rs9332096 | |
| 5′-Flanking | 15445429 | −1537 | AAGCAG/AAGGTA | | 247 | 16 | 0 | 0.030 | | [10,12,13,15–18] |
| 5′-Flanking | 15445778 | −1188 | ATCTT**T**/CTATTG | | 78 | 136 | 49 | 0.445 | rs4918758 | |
| 5′-Flanking | 15445985 | −981 | ATGGAG/AAAGGG | | 247 | 16 | 0 | 0.030 | rs9332098 | |
| 5′-Flanking | 15446081 | −885[a] | TTATGA/GACAGA | | 262 | 1 | 0 | 0.002 | | |
| 5′-Flanking | 15446234 | −732[a] | AGCTA**T**/GGAGCT | | 262 | 1 | 0 | 0.002 | | |
| Exon 1 | 15447014 | 49[a] | TTCTCC/ATTTCA | Leu17Ile | 262 | 1 | 0 | 0.002 | | |
| Intron 1 | 15447216 | IVS1+83 | GTACA**T**/CGTTAC | | 257 | 6 | 0 | 0.011 | rs9332104 | |
| Intron 1 | 15447258 | IVS1+125[a] | AGGCT**T**/CTTGTT | | 261 | 2 | 0 | 0.004 | | |
| Intron 1 | 15449977 | IVS1−164[a] | AGTGGC/AAAGTA | | 262 | 1 | 0 | 0.002 | | |
| Intron 1 | 15450031 | IVS1−110[a] | GCCTG**T**/GGTGG | | 260 | 3 | 0 | 0.006 | | |
| Intron 1 | 15450119 | IVS1−22[a] | TGCTG**T**/CTATCT | | 260 | 3 | 0 | 0.006 | | |
| Exon 2 | 15450200 | 228 | GTGGTG/ACTGCA | Val76Val | 260 | 3 | 0 | 0.006 | | [10] |
| Exon 2 | 15450241 | 269 | TGATC**T**/CTGGAG | Leu90Pro | 262 | 1 | 0 | 0.002 | | [11] |
| Intron 2 | 15450376 | IVS2+73 | AGAGC**T**/CCCTCG | | 257 | 6 | 0 | 0.011 | rs9332120 | |
| Exon 3 | 15450479 | 336[a] | GGAAT**T**/CGTTTT | Ile112Ile | 262 | 1 | 0 | 0.002 | | |
| Exon 3 | 15450496_15450505 | 353_362[a] | TGGAAA**GAAAT**GGAA/——GGAGA | Lys118Arg fsX9 | 262 | 1 | 0 | 0.002 | | |
| Exon 3 | 15450532 | 389[a] | CATGAC/GGCTGC | Thr130Arg | 262 | 1 | 0 | 0.002 | | |
| Exon 3 | 15450592 | 449[a] | AGCCCG/**T**CTGCC | Arg150Leu | 261 | 2 | 0 | 0.004 | | |
| Intron 3 | 15450821 | IVS3+197 | TGTGCG/**A**TACAG | | 188 | 67 | 8 | 0.158 | rs2860905 | |
| Intron 3 | 15450863 | IVS3+239 | TTCTCC/TTGAAC | | 133 | 109 | 21 | 0.287 | | [13] |
| Intron 3 | 15450889 | IVS3+265 | TCAAA**T**/CAAGAA | | 247 | 16 | 0 | 0.030 | | [13] |
| Intron 3 | 15455728 | IVS3−334 | CCTTGC/**T**TGTCT | | 188 | 68 | 7 | 0.156 | rs4086116 | |
| Intron 3 | 15455951 | IVS3−111[a] | TTGCT**G**/ATTAAG | | 262 | 1 | 0 | 0.002 | | |

Table 2 (Continued)

| Location | Position | | Nucleotide change and flanking sequences (5′–3′) | Amino acid change | Number of subjects | | | Allele Frequency | dbSNP SNP ID (NCBI) | Reference[c] |
|---|---|---|---|---|---|---|---|---|---|---|
| | NT_030059.12 | From the translational initiation site or from the end of nearest exon | | | Wild-type | Heterozygote | Homozygote | | | |
| Intron 3 | 15455997 | IVS3 – 65 | TATCTG/CTTAAC | | 202 | 56 | 5 | 0.125 | rs9332127 | |
| Exon 4 | 15456221 | 641[a] | GATCCA/TGGTAA | Gln214Leu | 262 | 1 | 0 | 0.002 | | |
| Intron 4 | 15456408 | IVS4 + 186[a] | AAATGC/TCTCAA | | 262 | 1 | 0 | 0.002 | | |
| Intron 4 | 15457276 | IVS4 – 115 | TCAAGA/GTATAC | | 202 | 56 | 5 | 0.125 | rs9332129 | |
| Exon 5 | 15457546 | 798[a] | GATTGC/TTTCCT | Cys266Cys | 262 | 1 | 0 | 0.002 | | |
| Intron 5 | 15457643 | IVS5 + 76[a] | TACTAA/GGGATG | | 262 | 1 | 0 | 0.002 | | |
| Intron 5 | 15480314 | IVS5 – 73 | TGTGAA/GTAATT | | 189 | 67 | 7 | 0.154 | rs9332172 | |
| Exon 6 | 15480402 | 835[a] | ACCAAC/ACATCT | Pro279Thr | 262 | 1 | 0 | 0.002 | | |
| Intron 6 | 15480623 | IVS6 + 95 | GCTTCA/GTTATT | | 257 | 6 | 0 | 0.011 | rs9332174 | |
| Intron 6 | 15480680 | IVS6 + 152[a] | TTACAA/GTGGGA | | 261 | 2 | 0 | 0.004 | | |
| Intron 6 | 15489303 | IVS6 – 163[a] | TTTGTG/ACATCTG | | 259 | 4 | 0 | 0.008 | | |
| Intron 6 | 15489329 | IVS6 – 137[a] | TTAAGT/ATTGCA | | 258 | 5 | 0 | 0.010 | | |
| Exon 7 | 15489579 | 1075 | ATACA/CTTGAC | Ile359Leu | 247 | 16 | 0 | 0.030 | rs1057910 | |
| Exon 7 | 15489641 | 1137[a] | AACTAT/CCTCAT | Tyr379Tyr | 260 | 3 | 0 | 0.006 | | |
| Intron 7 | 15489691 | IVS7 + 38 | GTTTTC/TGAAGT | | 245 | 18 | 0 | 0.034 | | [10] |
| Intron 8 | 15494510 | IVS8 + 53 | TTTTGA/TTCCAT | | 247 | 16 | 0 | 0.030 | rs9332230 | |
| Intron 8 | 15494604 | IVS8 + 147 | CCCTGC/TTCATG | | 133 | 109 | 21 | 0.287 | rs2298037 | |
| Intron 8 | 15497017 | IVS8 – 113[a] | TTCTAC/TGATAC | | 262 | 1 | 0 | 0.002 | | |
| Intron 8 | 15497018 | IVS8 – 112 | TCTACG/AATACA | | 247 | 16 | 0 | 0.030 | rs9332238 | |
| Intron 8 | 15497021 | IVS8 – 109 | ACGATA/TCACTG | | 75 | 136 | 52 | 0.456 | rs1934969 | |
| Intron 8 | 15497032 | IVS8 – 98[a] | AACAGT/ATATTG | | 262 | 1 | 0 | 0.002 | | |
| Exon 9 | 15497263 | 1425 | AATGGA/TTTTGC | Gly475Gly | 247 | 16 | 0 | 0.030 | rs1057911 | |
| Exon 9 | 15497267 | 1429[a] | GATTTG/ACCTCT | Ala477Thr | 262 | 1 | 0 | 0.002 | | |
| 3′-UTR | 15497318 | *7[a,b] | GAAGAG/CCAGAT | | 262 | 1 | 0 | 0.002 | | |
| 3′-UTR | 15497579_15497580 | *268_*269[b] | TTAATA/T–GTTAT | | 261 | 2 | 0 | 0.004 | | [12] |
| 3′-flanking | 15497707 | *396[b] | ATGCAT/AAATGT | | 247 | 16 | 0 | 0.030 | rs9332245 | |

[a]Novel variations detected in this study.
[b]The nucleotide following the translation termination codon TGA is numbered +1.
[c]Refer to the reference section.

**Fig. 1**

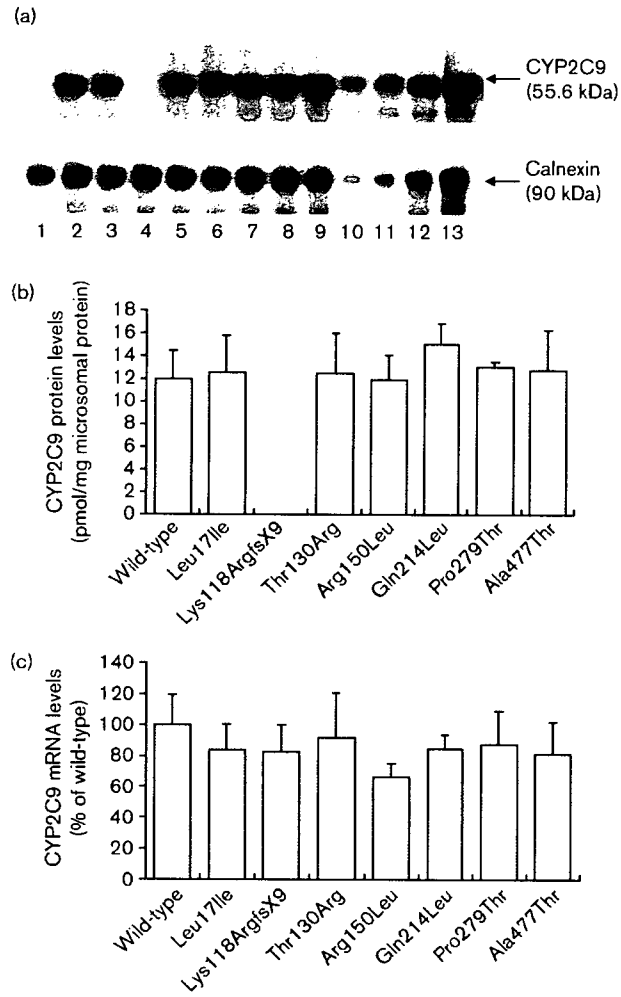


Expression of wild-type and seven variant CYP2C9 in COS-1 cells. (a) A representative Western blot showing the immunoreactive proteins for CYP2C9 (upper panel) and for calnexin (lower panel). Lane 1, empty vector; lane 2, wild-type; lane 3, Leu17Ile; lane 4, Lys118ArgfsX9; lane 5, Thr130Arg; lane 6, Arg150Leu; lane 7, Gln214Leu; lane 8, Pro279Thr; lane 9, Ala477Thr; lanes 10–13, commercially available CYP2C9-expressed microsomes used for calibration standards, 0.1 pmol P450 (lane 10), 0.2 pmol P450 (lane 11), 0.5 pmol P450 (lane 12) and 0.75 pmol P450 (lane 13). (b) Quantitative results of immunoreactive CYP2C9 protein. Each bar represents the mean ± SD of three separate experiments. (c) Quantitative results of CYP2C9 mRNA expression assessed by TaqMan real-time reverse transcriptase-polymerase chain reaction. Each sample was normalized to β-actin mRNA content and expressed as a percentage of wild-type. Each bar represents the mean ± SD of four to six separate experiments.

CYP2C9 mRNA expression levels were determined by TaqMan real-time RT-PCR (Fig. 1c). CYP2C9 mRNA was not detected from cells transfected with the empty plasmid. CYP2C9 mRNA levels in the seven variants were not significantly different from those in the wild-type ($P = 0.22$), suggesting that the transfection/transcription efficiencies of all plasmid constructs were nearly equal. Therefore, the truncated protein derived from the Lys118ArgfsX9 variant might be unstable and/or rapidly degraded in this expression system.

### Diclofenac 4′-hydroxylation activities of the wild-type and seven variant CYP2C9s

Figure 2 shows the Michaelis–Menten curves for diclofenac 4′-hydroxylation by the wild-type and six variants. As expected, no 4′-hydroxylated metabolite was detected for the microsomal preparation derived from the Lys118ArgfsX9 variant (data not shown). The kinetic parameters are summarized in Table 3. The $K_m$ value (13.2 ± 1.0 μM) of the wild-type was comparable to those of human liver microsomes (5.6–27.6 μM) [22,27], but slightly higher than those previously reported for yeast-expressed CYP2C9 (1.8–3.9 μM) [5,28] and CYP2C9 expressed in a baculovirus/insect system (4.8 μM) [8]. The relatively rapid depletion of diclofenac at lower concentrations (2.5–10 μM) might have occurred in our experimental conditions and resulted in the elevated $K_m$ value of the wild-type (underestimation of the enzyme activity). The $V_{max}$ value (32.1 ± 2.4 pmol/min/pmol CYP2C9) of wild-type was also comparable to that previously reported for yeast-expressed CYP2C9 (35.6 ± 1.3 pmol/min/pmol P450) [28].

As shown in Table 3, the Thr130Arg variant was the most defective in metabolizing diclofenac among the six variants. The $V_{max}$ value and intrinsic clearance were significantly decreased by 93% and 83%, respectively, both on the mg microsomal protein basis and pmol CYP2C9 basis ($P < 0.01$ for all comparisons to the

**Fig. 2**

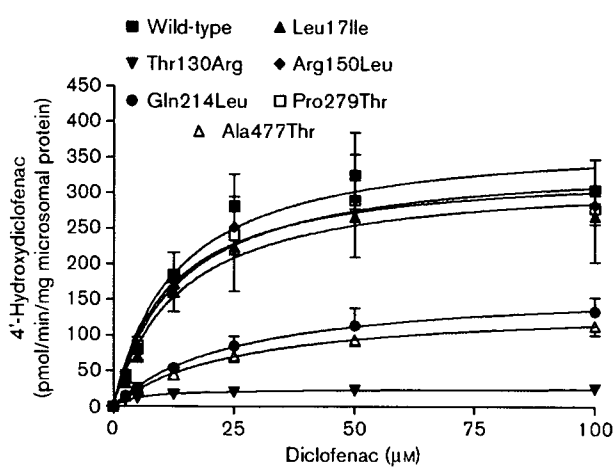


Michaelis–Menten curves for diclofenac 4′-hydroxylation from recombinant wild-type and variant CYP2C9. The solid line indicates fitting of the data to the Michaelis–Menten equation by non-linear regression. Each point represents the mean ± SD of three independent preparations derived from different transfections.

Table 3 Kinetic parameters for hydroxylation activities of wild-type and variant CYP2C9 against diclofenac

| Amino acid alteration | $K_m$ (μM) | $V_{max}$ (pmol/min/mg protein) | $V_{max}$ (pmol/min/pmol P450) | Clearance ($V_{max}/K_m$) (μl/min/mg protein) | Clearance ($V_{max}/K$) (μl/min/pmol P450) |
|---|---|---|---|---|---|
| Wild-type | 13.2±1.0 | 381.7±59.9 | 32.1±2.4 | 29.1±5.3 | 2.4±0.09 |
| Leu17Ile | 13.7±2.6 | 326.0±85.3 | 27.9±11.5 | 23.6±2.9 | 2.0±0.52 |
| Lys118ArgfsX9 (*25) | ND | ND | ND | ND | ND |
| Thr130Arg (*26) | 5.9±2.0 | 25.9±6.0**** | 2.2±0.7** | 4.7±1.8**** | 0.4±0.22**** |
| Arg150Leu (*27) | 13.4±3.2 | 351.2±86.8 | 31.0±11.8 | 26.1±0.4 | 2.2±0.43 |
| Gln214Leu (*28) | 25.9±4.5*** | 170.6±31.3* | 11.5±2.4 | 6.7±1.3**** | 0.5±0.13**** |
| Pro279Thr (*29) | 11.9±2.7 | 338.1±34.7 | 26.0±3.0 | 29.0±4.4 | 2.2±0.37 |
| Ala477Thr (*30) | 25.9±0.7*** | 142.9±14.7** | 11.7±2.5 | 5.5±0.6**** | 0.5±0.10**** |

*$P<0.05$,
**$P<0.01$,
***$P<0.005$
****$P<0.001$ versus wild-type. One-way analysis of variance, post-hoc test; Scheffe. Data is represented by mean±SD. ND, Not detected.

wild-type). By contrast, its $K_m$ value was not significantly changed. The two variants, Gln214Leu and Ala477Thr, both of which were also defective compared to the wild-type, showed similar kinetics. The $K_m$ values of these two variant enzymes were approximately two-fold higher than that of the wild-type ($P < 0.005$). They also exhibited 55% (Gln214Leu) and 63% (Ala477Thr) decrease in $V_{max}$ and 77% (Gln214Leu) and 81% (Ala477Thr) decrease in intrinsic clearance ($V_{max}/K_m$) on the basis of mg microsomal protein, and these reductions were statistically significant. After normalization to the corresponding CYP2C9 protein content determined by Western blotting, the intrinsic clearance of both Gln214Leu and Ala477Thr was still significantly lower than that of the wild-type ($P < 0.001$). The kinetic parameters of other variants (Leu17Ile, Arg150Leu and Pro279Thr) were similar to those of the wild-type. Thus, these results demonstrate that in addition to the Lys118ArgfsX9 variant, the three amino acid substitution variants, Thr130Arg, Gln214Leu and Ala477Thr, cause markedly decreased catalytic activities towards diclofenac hydroxylation *in vitro*.

### LD analysis

Using 26 common SNPs (more than 0.01 in their allele frequencies), LD analysis was performed by $|D'|$ and $r^2$ statistics, and their pairwise values are depicted with a 10-graded blue colour in Fig. 3. As already reported in various ethnic groups [10,12,13,16], five SNPs, −1911T > C, −1885C > G, −1537G > A, −981G > A, IVS3 + 265T > C and IVS8 + 53A > T, were in perfect LD ($r^2 = 1.0$) with 1075A > C (*3, Ile359Leu). Furthermore, we found that an additional three SNPs, IVS8-112G > A, 1425A > T (Gly475Gly) and *396T > A, were also perfectly associated with *3 in Japanese ($r^2 = 1.0$). Veenstra *et al.* [13] also reported that IVS8−112G > A was linked both with *2 and *3 in European-American warfarin patients; however, *2 (430C > T, Arg144Cys) was not detected in our study.

Perfect LD was observed in four other variation pairs: −3089G > A and −2665_−2664delTG; −1565C > T, IVS3−65G > C and IVS4−115A > G; IVS1 + 83T > C, IVS2 + 73T > C and IVS6 + 95A > G; and IVS3 + 239C > T and IVS8 + 147C > T. Close associations were observed among −1565C > T, IVS3 + 197 G > A, IVS3−334C > T, IVS3−65G > C, IVS4−115A > G and IVS5−73A > G ($r^2 = 0.76$) and among −3089G > A, −2665_−2664delTG, −1188T > C, IVS3 + 239C > T, IVS8 + 147C > T and IVS8−109A > T ($r^2 > 0.48$).

As for the $|D'|$ values between 26 common SNPs, 283 pairs (87%) and 311 pairs (95%) out of 325 pairs had $|D'| > 0.99$ and $|D'| > 0.80$, respectively, indicating that one LD block covers the entire gene. Recombination might have occurred between −2665_−2664delTG and −1911T > C in four out of 263 subjects (data not shown), but this event was too minor to divide the LD block. Thus, the haplotypes of *CYP2C9* were analysed as one LD block that spans at least 54 kb.

### Haplotype estimation, selection of haplotype-tagging SNPs and network analysis

Using all 62 SNPs detected, 46 haplotypes were inferred. Although a large number of haplotypes were inferred, they were classified into only six major haplotype groups: *1A, *1B, *1e, *1f, *1h and *3 groups as shown in Fig. 4. The probability of diplotype configurations was over 0.99 except for 12 subjects.

The *1A group of haplotypes consisted of 15 *1 subtypes and three haplotypes with non-synonymous SNPs, *25a (Lys118ArgfsX9), *28a (Gln214Leu) and *30a (Ala477Thr). The most dominant haplotype *1A (frequency = 0.489) without nucleotide changes was considered the wild-type haplotype. The other haplotypes in this group differ from *1A in only one site and were found at frequencies of ≤ 0.01.

The *1B group was defined as the group of haplotypes that contained six linked non-coding SNPs, −3089G > A, −2665_−2664delTG, −1188T > C, IVS3 + 239C > T, IVS8 + 147C > T and IVS8−109A > T. The second

**Fig. 3**

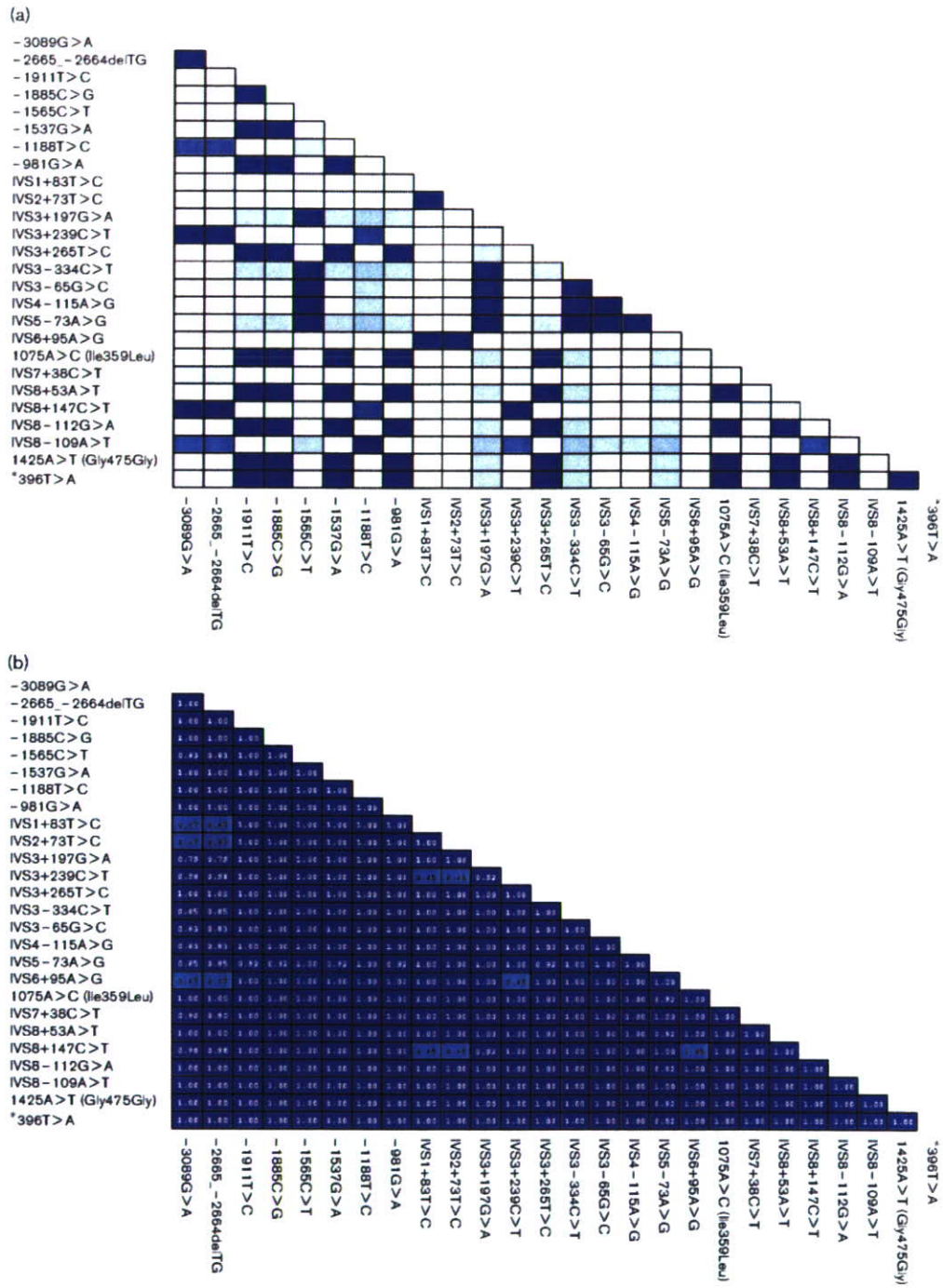


**Linkage disequilibrium (LD) analysis of *CYP2C9*. Pairwise LD between 26 common single nucleotide polymorphisms (>0.01 in allele frequencies) is expressed as (a) $r^2$ and (b) |D'| by a 10-graded blue colour. The denser colour indicates higher linkage.**

common haplotype in Japanese, ***1B*** (0.222 in frequency), was the most dominant haplotype in this group. This haplotype, first assigned as ***1B*** by King *et al.* [16], was reported by Veenstra *et al.* [13] as Haplotype 6 (***1B***). This group included the other 11 ***1*** subtypes, ***13a*** (Leu90Pro) and ***27a*** (Arg150Leu), with frequencies less than 0.01.

The ***1e*** group consisted of four haplotypes, ***1e***, ***1p***, ***1ac*** and ***26a*** (Thr130Arg), all of which were characterized by